OXFORD

Cerebral Cortex, 2022, 1–19
https://doi.org/10.1093/cercor/bhac018
Original Article

Replicable patterns of causal information flow between hippocampus and prefrontal cortex during spatial navigation and spatial–verbal memory formation

Anup Das [1,*], Vinod Menon[1,2,3,*]

[1]Department of Psychiatry and Behavioral Sciences, Stanford University School of Medicine, Stanford, CA 94305, USA,
[2]Department of Neurology and Neurological Sciences, Stanford University School of Medicine, Stanford, CA 94305, USA,
[3]Stanford Neurosciences Institute, Stanford University School of Medicine, Stanford, CA 94305, USA

*Corresponding author: Email: a1das@stanford.edu (AD), menon@stanford.edu (VM)

Abstract

Interactions between the hippocampus and prefrontal cortex (PFC) play an essential role in both human spatial navigation and episodic memory, but the underlying causal flow of information between these regions across task domains is poorly understood. Here we use intracranial EEG recordings and spectrally resolved phase transfer entropy to investigate information flow during two different virtual spatial navigation and memory encoding/recall tasks and examine replicability of information flow patterns across spatial and verbal memory domains. Information theoretic analysis revealed a higher causal information flow from hippocampus to lateral PFC than in the reverse direction. Crucially, an asymmetric pattern of information flow was observed during memory encoding and recall periods of both spatial navigation tasks. Further analyses revealed frequency specificity of interactions characterized by greater bottom-up information flow from hippocampus to PFC in delta–theta band (0.5–8 Hz); in contrast, top-down information flow from PFC to hippocampus was stronger in beta band (12–30 Hz). Bayesian analysis revealed a high degree of replicability between the two spatial navigation tasks (Bayes factor > 5.46e+3) and across tasks spanning the spatial and verbal memory domains (Bayes factor > 7.32e+8). Our findings identify a domain-independent and replicable frequency-dependent feedback loop engaged during memory formation in the human brain.

Key words: human intracranial electroencephalography; hippocampal–prefrontal cortex information flow; phase transfer entropy; episodic memory; spatial navigation and memory.

1. Introduction

In rodents, nonhuman primates, and humans alike, the hippocampus and prefrontal cortex (PFC) both play essential roles in spatial navigation and memory formation (Eichenbaum 2017; Ekstrom et al. 2017; Herweg and Kahana 2018; Rutishauser et al. 2021). The hippocampus is a critical brain region for remembering the location of objects in space (Burgess et al. 2002). Extensive research on the neurophysiology of spatial memory in rodents has revealed the presence of hippocampal place cells, which increase their firing rate when an animal passes through a specific location in the environment (O'Keefe and Conway 1978). Individual neurons in the hippocampus also encode an animal's spatial location with respect to landmarks and spatial boundaries (Eichenbaum et al. 1999; Hartley et al. 2014). There is now substantial evidence that the hippocampus does not function in isolation and that its feedforward and feedback interactions with the PFC are essential for encoding and recall of spatial information via cognitive and strategic control over memory formation processes (Moscovitch 1992; Buckner and Wheeler 2001; Miller and Cohen 2001; Dobbins et al. 2002; Postle 2006). However, the temporal and causal dynamics of these processes, and similarities across tasks and spatial–verbal domains, are poorly understood. Here, we use data from a large cohort of intracranial EEG (iEEG) recordings and multiple tasks to investigate information flow between the hippocampus and distinct subdivisions of the PFC, its frequency specificity, and replicability across task domains, during memory encoding and recall during spatial navigation as well as verbal recall.

Electrophysiological studies in rodents have reported strong delta (0.5–4 Hz) and theta (4–8 Hz) frequency band oscillations in the hippocampus (Siapas et al. 2005; Eichenbaum 2017; Roy et al. 2017; Schultheiss et al. 2020). Rodent electrophysiological studies have also revealed synchronized activity between the hippocampus and PFC in these frequency bands during spatial memory tasks (Simons and Spiers 2003; Jones and Wilson 2005; Benchenane et al. 2010; Place et al. 2016; Spiers 2020). Research has also shown that theta oscillations in the hippocampus play a role in both encoding and retrieval of spatial information from memory (Buzsáki 2005;

Received: November 16, 2021. **Revised:** January 11, 2022. **Accepted:** January 13, 2022

Herweg and Kahana 2018). Moreover, theta rhythms have been widely implicated in rodent hippocampal function, and theta band coherence and phase-locked spiking within both the hippocampus and PFC have been implicated in spatial memory–guided behavior (Zielinski et al. 2019). Studies in rodents have also shown that hippocampal–PFC theta local field potential coherence increases during learning (Benchenane et al. 2010).

In contrast, there is much less information available about the electrophysiological basis of dynamic causal signaling between the hippocampus and PFC during spatial navigation and memory formation in the human brain. Furthermore, it is not known whether feedforward and feedback interactions of the PFC with the hippocampus are symmetric and frequency specific. Functional MRI studies in humans have consistently demonstrated that both the hippocampus and PFC are coactivated during spatial navigation, but the temporal dynamics and frequency specificity of their interactions remain unknown because of the poor temporal resolution of fMRI. In humans, iEEG studies of spatial navigation and memory recall have primarily focused on the hippocampus and few studies have directly examined their interactions and signal flow between these regions. Studies using simultaneous fMRI–EEG (Neuner et al. 2014) and iEEG (Watrous et al. 2013; Ekstrom and Watrous 2014) and single neuron studies have also reported that cells throughout the frontal and temporal lobes respond to navigational goals and to conjunctions of place, goal, and view (Ekstrom et al. 2003). Ekstrom et al. have hypothesized that increased coherence between the hippocampus and the PFC in low frequency may play a foundational role in spatial memory–related behaviors in both rodents and humans (Ekstrom and Watrous 2014), but studies have yet to identify its specific neurophysiological basis. More research within multiple datasets is therefore needed to identify replicable neural mechanisms underlying signaling between hippocampus and PFC regions that underlie memory formation and thereby fill a major gap between rodent and human neurophysiological studies.

Although studies to date have provided insights into the involvement of both the hippocampus and PFC in human spatial navigation and memory, the precise pattern of "bottom-up" and "top-down" dynamic causal interactions and frequency-dependent direction of information flow are not known due to the poor temporal resolution of fMRI and the paucity of simultaneous electrophysiological data from the hippocampus and multiple PFC regions. To address this challenge, we used iEEG data from the UPENN-RAM study (Solomon et al. 2019), which includes depth recordings from a large cohort of individuals, to probe the directionality of information flow between the hippocampus and multiple subdivisions of the lateral PFC implicated in cognitive control across multiple virtual spatial navigation tasks.

The first goal of our study was to determine causal information flow between the hippocampus and the PFC during spatial memory processing. We used two virtual spatial memory tasks: The Treasure Hunt spatial navigation task and the Water Maze spatial navigation task. Both tasks consisted of multiple trials of encoding and recall periods. In both tasks, participants were shown objects in various locations during the encoding periods; during the recall period, they were asked to retrieve the location of the objects. We used phase transfer entropy (PTE) to investigate information flow between hippocampus and distinct PFC regions during memory encoding and recall periods in the two spatial navigation tasks (Lobier et al. 2014; Hillebrand et al. 2016; Wang et al. 2017). PTE provides a robust and powerful measure for characterizing information flow between brain regions based on phase coupling, and crucially, it captures linear as well as nonlinear intermittent and nonstationary causal dynamics in iEEG data (Menon et al. 1996; Lobier et al. 2014; Hillebrand et al. 2016).

We build on our recent work on the role of the left hippocampus and left PFC in verbal memory encoding and recall (Das and Menon 2021) and determine if the same dynamical processes also hold and replicate across multiple spatial navigation tasks. We examined nonlinear causal interactions between hippocampus and lateral PFC using intracranial EEG recordings during verbal memory encoding and recall tasks. Direction-specific information theoretic analysis revealed higher causal information flow from the hippocampus to PFC than in the reverse direction. Crucially, this pattern was observed during both memory encoding and recall, and the strength of causal interactions was significantly greater during memory task performance than resting baseline. Whether similar dynamic information flow occurs in a domain-independent manner across spatial and verbal memory tasks is not known.

The role of left hemisphere hippocampus–PFC circuits during spatial navigation and memory formation has generally received less attention in the literature. Although several lesion studies in humans have demonstrated the role of the right hemisphere hippocampus in spatial memory formation (Smith and Milner 1989; Abrahams et al. 1997; Spiers et al. 2001; Burgess et al. 2002), the role of the left hemisphere in spatial navigation and memory in humans has been less clear, with some lesion studies also pointed to the involvement of both the left and right hemisphere hippocampus in spatial memory (Maguire et al. 1996; Bohbot et al. 1998; Spiers et al. 2001). Recent evidence using iEEG recordings in humans performing virtual (Miller et al. 2018) as well as real-world (Stangl et al. 2021) spatial navigation tasks, object–location memory tasks (Stevenson et al. 2018), and single neuron recordings in humans performing virtual spatial navigation tasks (Jacobs et al. 2013) has shown that the left hemisphere hippocampus may also play a crucial role for spatial memory encoding. Here

we take advantage of extensive left-hemisphere iEEG recordings to investigate dynamic causal circuits in the left hemisphere hippocampus interactions with two distinct PFC areas that encompass the middle frontal gyrus (MFG) and the inferior frontal gyrus (IFG). Based on the hypothesized role of the hippocampus in memory encoding, we test the prediction that causal influences of the hippocampus on the PFC would be stronger, compared with the reverse direction, during memory encoding. In contrast, based on the hypothesized role of the PFC in controlled memory retrieval, we test the hypothesis that causal influences of the PFC on the hippocampus would be stronger, compared with the reverse direction, during memory recall (Hasegawa et al. 1999; Wagner et al. 2001; Dobbins et al. 2002; Badre et al. 2005; Badre and Wagner 2007).

Our second goal was to investigate the frequency specificity of causal interactions between the hippocampus and the PFC. The role of specific frequencies in synchronization of neural responses between the hippocampus and PFC (Brincat and Miller 2015; Moreno et al. 2016) in rodents, nonhuman primates, and humans is still poorly understood, but emerging findings point to differential engagement of delta–theta rhythm (0.5–8 Hz) in the hippocampus (Watrous et al. 2013; Ekstrom and Watrous 2014; Neuner et al. 2014) in contrast to beta-band rhythm (12–30 Hz) in prefrontal and parietal cortices (Brovelli et al. 2004; Engel and Fries 2010; Spitzer and Haegens 2017; Stanley et al. 2018).

Our analyses of data from the UPENN-RAM consortium in participants performing a verbal memory encoding and recall tasks revealed frequency specificity of interactions with greater causal information flow from hippocampus to the PFC in the delta–theta frequency band (0.5–8 Hz); in contrast, PFC to hippocampus causal information flow was stronger in the beta band (12–30 Hz). Thus, we hypothesized that delta–theta oscillations would preferentially contribute to the synchronization of the hippocampus with the PFC (Ekstrom and Watrous 2014), while beta-band oscillations synchronize the PFC with other cortical and subcortical brain areas (Engel and Fries 2010; Spitzer and Haegens 2017; Negrón-Oyarzo et al. 2018).

Our final goal was to investigate the replicability of our findings across multiple memory tasks. Replicating findings across multiple datasets is an extremely challenging problem in neuroscience and especially difficult for invasive iEEG studies. To the best of our knowledge, no human iEEG studies have replicated findings across multiple memory tasks, and quantitatively rigorous measures are needed to address the reproducibility crisis in human iEEG studies. To accomplish this, we used Bayesian analysis to quantify the degree of replicability (Verhagen and Wagenmakers 2014; Ly et al. 2019). Bayes factors (BFs) are a powerful tool for evaluating evidence for replicability of findings across tasks and for determining the strength of evidence for the null hypothesis (Verhagen and Wagenmakers 2014). Briefly, the replication BF is the ratio of marginal likelihood of the replication data given the posterior distribution estimated from the original data and the marginal likelihood for the replication data under the null hypothesis of no effect (Ly et al. 2019). We first computed the replication BF between the Treasure Hunt (original) and Water Maze (replication) spatial memory tasks and then across tasks spanning our original verbal (Das and Menon 2021), and the present spatial, memory domains.

Our analysis revealed novel insights into the neurophysiological basis of human hippocampal–PFC interactions and its role in both memory encoding and recall across multiple spatial navigation tasks. Our findings also address the reproducibility challenge in iEEG research and systems neuroscience by demonstrating a high replication BF within and across domains.

2. Materials and methods

2.1 UPENN-RAM iEEG recordings

iEEG recordings from 249 patients shared by Kahana and colleagues at the University of Pennsylvania (UPENN) (obtained from the UPENN-RAM public data release) were used for analysis (Jacobs et al. 2016). Patients with pharmaco-resistant epilepsy underwent surgery for removal of their seizure onset zones. The iEEG recordings of these patients were downloaded from a data-sharing archive hosted by the UPENN-RAM consortium (URL: http://memory.psych.upenn.edu/RAM). Before data collection, the Institutional Review Board approved research protocols and ethical guidelines at participating hospitals, and informed consent was obtained from participants and guardians (Jacobs et al. 2016). Details of all the recording sessions and data preprocessing procedures are described by Kahana and colleagues (Jacobs et al. 2016). Briefly, iEEG recordings were obtained using subdural grids and strips (contacts placed 10 mm apart) or depth electrodes (contacts spaced 5–10 mm apart) using recording systems at each clinical site. The iEEG systems included DeltaMed XlTek (Natus), Grass Telefactor, and Nihon-Kohden EEG systems. Electrodes located in brain lesions or those that corresponded to zones of onset of seizures or had significant interictal spiking or had broken leads were excluded from the analysis.

Anatomical location of electrode placement was accomplished by coregistering postoperative computed tomography with postoperative magnetic resonance imaging using software packages FSL (FMRIB (Functional MRI of the Brain), Brain Extraction Tool (BET), and FMRIB Linear Image Registration Tool (FLIRT). Preoperative magnetic resonance imaging was used when postoperative magnetic resonance imaging was not available. The resulting contact locations were mapped to the MNI space using an indirect stereotactic technique and the OsiriX Imaging Software DICOM viewer package. We used the Brainnetome atlas (Fan et al. 2016) to demarcate the left hemisphere MFG, IFG, and the

hippocampus (Greicius et al. 2003). In our analysis, MFG, IFG, and the hippocampus in the right hemisphere were not considered due to the lack of sufficient electrode placement in the right hemisphere. Other important brain regions, such as the anterior dorsal cingulate cortex (dACC) and the medial dorsal prefrontal cortex (dmPFC), were also excluded from the analysis due to the lack of adequate electrode placement in these areas. Out of 249 individuals, data from 40 individuals (aged 19–66, mean age 33.8 ± 11.1, 22 females) were used for subsequent analysis based on electrode placement in MFG, IFG, and the hippocampus and based on the types of tasks the subjects performed (apart from spatial navigation tasks, subjects also performed verbal free recall tasks; see http://memory.psych.upenn.edu/RAM for more details; also see Das and Menon 2021). Gender differences were not analyzed in this study due to the lack of sufficient male participants for electrode pairs for hippocampus–IFG interactions (Supplementary Table 2).

The original sampling rates of the iEEG signals were 500, 999, 1000, 1600, and 2000 Hz. Therefore, the iEEG signals were downsampled to 500 Hz, if the original sampling rate was higher, for all subsequent analyses. The two main concerns when analyzing interactions between closely spaced intracranial electrodes are volume conduction and confounding interactions with the reference electrode (Burke et al. 2013). Therefore, bipolar reference was used to eliminate confounding artifacts and improve the signal-to-noise ratio of neural signals, consistent with previous studies using UPENN-RAM iEEG data (Burke et al. 2013; Ezzyat et al. 2018). The signals recorded on individual electrodes were converted to a bipolar montage by computing the difference in signal between adjacent electrode pairs on each strip, grid, and depth electrode, and the resulting bipolar signals were treated as new "virtual" electrodes originating from the midpoint between each contact pair, identical to procedures in previous studies using UPENN-RAM data (Solomon et al. 2019). Line noise (60 Hz) and its harmonics were removed from the bipolar signals, and finally each bipolar signal was Z normalized by removing mean and scaling by the standard deviation. For filtering, we used a fourth-order two-way zero phase lag Butterworth filter throughout the analysis.

2.2 iEEG spatial navigation tasks

2.2.1 Treasure Hunt spatial navigation task

The patients performed multiple trials of a spatial memory task in a virtual reality environment developed in Unity3D (Miller et al. 2018; Tsitsiklis et al. 2020), where they played a Treasure Hunt task on a laptop computer at the bedside and controlled their translational and rotational movements through the virtual environment with a handheld joystick. In each task trial, subjects explored a rectangular arena on a virtual 3D beach to reach treasure chests that revealed hidden objects, with the goal of encoding the location of each item encountered (Fig. 2a). The virtual beach (100 × 70 virtual units, 1.42: 1 aspect ratio) was bounded by a wooden fence on each side. The locations of the objects changed over the trials, but the shape, size, and appearance of the environment remained constant throughout the sessions. The task environment was constructed so that the subject would perceive one virtual unit as corresponding to ∼1 foot in the real world. Subjects viewed the environment from the perspective of cycling through the environment and the elevation of their perspective was 5.6 virtual units. Each end of the environment had unique visual cues to help the subjects navigate.

Each trial of the task begins with the subject being placed on the ground at a randomly selected end of the environment. The subject initiates the trial with a button press and then navigates to a chest using a joystick. Upon arrival at the chest, the chest opens and either reveals an object, which the subject should try to remember, or is empty. The subject remains facing the open chest for 1.5 s ("encoding period") and then the object and chest disappear, which indicates that the subject should navigate to the next chest that has now appeared in the arena. Each trial consists of four chests; two or three (randomly selected, so that subjects could not predict whether the current target chest contained an object, which served to remove effects of expectation and to encourage subjects to always attend to their current location as they approached a chest) of the chests contain an object, and the others are empty. Each session consists of 40 trials, and in each session, subjects visit a total of 100 full chests and 60 empty chests. The chests are located pseudorandomly throughout the interior of the environment, subject to the restrictions that no chest can be placed within 11 virtual units of another and that all chests must be at least 13 virtual units from the arena boundary. This 11 virtual unit restriction ensures that chest locations are varied in a trial. There are no constraints based on previous trials, and all object identities are trial-unique and never repeated within a session. After reaching all four chests of a trial, subjects are transported automatically so that they have an elevated 3/4 overhead perspective view of the environment at a randomly selected end of the environment. The reason for this perspective shift was to speed up the recall period, preserving patient testing time to provide a relatively larger number of memory encoding events. They then perform a distractor task, a computerized version of the "shell game," before entering the "recall period." During recall, subjects are cued with each of the objects from the trial in a random sequence and asked to recall the location of the object. In each recall period, they first indicate their confidence to remember the location of the object ("high," "medium," or "low"). Next, they indicate the precise location of the object by placing a cross-hair at the location in the environment that corresponds to the location of the cued item. After the location of each object of the trial is indicated, the feedback stage of each trial begins. Here, subjects are shown their response for each cued object in the trial, via a green circle if the

location was correct and a red circle if it was incorrect. Subjects receive feedback on their performance, following a point system where they receive greater rewards for accurate responses. A response is considered correct if it is within 13 virtual units of the true object location.

Only trials corresponding to successful memory encoding and recall are considered in our analysis. From the point of view of probing behaviorally effective memory encoding, our focus was therefore on successful recall consistent with most prior studies (Watrous et al. 2013; Long et al. 2014). We analyzed 1.5-s iEEG epochs from the encoding and recall periods of the Treasure Hunt task. Data from each trial were analyzed separately and specific measures were averaged across trials.

2.2.2 Water Maze spatial navigation task

Similar to the Treasure Hunt task, patients performed multiple trials of a spatial memory task in a virtual navigation paradigm (Jacobs et al. 2016; Goyal et al. 2018; Lee et al. 2018) similar to the Morris Water Maze (Morris 1984). The environment was rectangular (1.8:1 aspect ratio) and was surrounded by a continuous boundary (Fig. 2b). There were four distal visual cues (landmarks), one centered on each side of the rectangle, to aid in orienting. Each trial (96 trials per session, 1–3 sessions per subject) started with two 5-s "encoding periods," during which subjects were driven to an object from a random starting location. At the beginning of an encoding period, the object appeared, and, over the course of 5 s, the subject was automatically driven directly toward it. The 5-s period consisted of three intervals: first, the subject was rotated toward the object (1 s); second, the subject was driven toward the object (3 s); and finally, the subject paused while at the object location (1 s). After a 5-s delay with a blank screen, the same process was repeated from a different starting location. After both encoding periods for each item, there was a 5-s pause followed by the "recall period." The subjects was placed in the environment at a random starting location with the object hidden and then asked to freely navigate using a joystick to the location where they thought the object was located. When they reached their chosen location, they pressed a button to record their response. They then received feedback on their performance via an overhead view of the environment showing the actual and reported object locations.

Similar to the Treasure Hunt spatial navigation task, only trials corresponding to successful memory encoding and recall are considered in our analysis. We analyzed 5-s iEEG epochs from the encoding and recall periods of the task. Data from each trial were analyzed separately and specific measures were averaged across trials, similar to the Treasure Hunt spatial navigation task.

2.3 iEEG analysis of power spectral density

To calculate average power, we first filtered the iEEG time series in the frequency band of interest, and power, after removing the linear trend, was calculated as the sum of the squares of the amplitudes of the iEEG time series divided by the length of the time series.

2.3.1 iEEG analysis of PTE and causal dynamics

PTE is a nonlinear measure of the directionality of information flow between time series and can be applied as a measure of causality to nonstationary time series (Lobier et al. 2014). Note that the information flow described here relates to signaling between brain areas and does not necessarily reflect the representation or coding of behaviorally relevant variables per se. The PTE measure is in contrast to the Granger causality measure, which can be applied only to stationary time series (Barnett and Seth 2014). We first carried out a stationarity test of the iEEG recordings (unit root test for stationarity; Barnett and Seth 2014) and found that the spectral radius of the autoregressive model is very close to one, indicating that the iEEG time series is nonstationary. This precluded the applicability of the Granger causality analysis in our study.

Given two time series $\{x_i\}$ and $\{y_i\}$, where $i = 1, 2, \ldots, M$, instantaneous phases were first extracted using the Hilbert transform. Let $\{x_i^p\}$ and $\{y_i^p\}$, where $i = 1, 2, \ldots, M$, denote the corresponding phase time series. If the uncertainty of the target signal $\{y_i^p\}$ at delay τ is quantified using Shannon entropy, then the PTE from driver signal $\{x_i^p\}$ to target signal $\{y_i^p\}$ can be given by

$$\mathrm{PTE}_{x\to y} = \sum_i p\left(y_{i+\tau}^p, y_i^p, x_i^p\right) \log\left(\frac{p\left(y_{i+\tau}^p | y_i^p, x_i^p\right)}{p\left(y_{i+\tau}^p | y_i^p\right)}\right), \quad (1)$$

where probabilities can be calculated by building histograms of occurrences of singles, pairs, or triplets of instantaneous phase estimates from the phase time series (Hillebrand et al. 2016). For our analysis, the number of bins in the histograms was set as $3.49 \times \mathbf{STD} \times M^{-1/3}$ and delay τ was set as $2M/M_{\pm}$, where **STD** is average standard deviation of the phase time series $\{x_i^p\}$ and $\{y_i^p\}$ and $M_{\pm}$ is the number of times the phase changes sign across time and channels (Hillebrand et al. 2016). Across all pairs of hippocampus–PFC electrodes, the propagation delay between source and target signals was estimated to be 25.8 ms, which is physiologically significant and corresponds to directional signal interactions on a timescale consistent with monosynaptic influence (see Das and Menon 2021, for a detailed discussion of this). PTE has been shown to be robust against the choice of the delay τ and the number of bins for forming the histograms (Hillebrand et al. 2016). Because PTE requires a large number of samples for estimating histograms of the conditional probabilities (Hillebrand et al. 2016; Wang et al. 2017), time-resolved analysis of dynamic changes in causal interactions could not be performed. In the present study, we used ~1.5-s epochs from the Treasure Hunt task and ~5-s epochs from the Water Maze task with 500-Hz sampling rate (see above), which are similar to iEEG epochs used in other iEEG studies

(Wang et al. 2017) and considerably shorter than 300 s used in magnetoencephalography studies (Hillebrand et al. 2016).

2.4 Statistical analysis

Statistical analysis was performed using mixed effects analysis with the lmerTest package (Kuznetsova et al. 2017) implemented in R software (version 4.0.2, R Foundation for Statistical Computing). Because PTE data were not normally distributed, we used BestNormalize (Peterson and Cavanaugh 2018), which contains a suite of transformation estimation functions that can be used to optimally normalize data. The resulting normally distributed data were subjected to mixed effects analysis with the following model: PTE ~ Condition + (1|Subject), where *Condition* models fixed effects (condition differences) and (1|*Subject*) models random repeated measurements within the same participant. Analysis of variance (ANOVA) was used to test the significance of the findings with FDR corrections for multiple comparisons ($P < 0.05$). Similar mixed effects statistical analysis procedures were used for comparison of power spectral density across task conditions.

2.4.1 Surrogate data analysis

We conducted surrogate analysis to test the significance of the estimated PTE values (Hillebrand et al. 2016) and whether the observed effects are beyond chance levels. The estimated phases from the Hilbert transform for electrodes from a given pair of brain areas were time-shuffled so that the predictability of one time series from another is destroyed, and PTE analysis was repeated on this shuffled data to build a distribution of surrogate PTE values against which the observed PTE was tested ($P < 0.05$).

2.4.2 Bayesian replication analysis

Finally, we used replication BF (Verhagen and Wagenmakers 2014; Ly et al. 2019) analysis to estimate the degree of replicability for the direction of information flow for each frequency and task condition and across the two spatial memory tasks. Analysis was implemented in R software using the BayesFactor package (Rouder et al. 2009). Because PTE data were not normally distributed, as previously, we used BestNormalize (Peterson and Cavanaugh 2018) to optimally normalize data. We compared the BF of the joint model $PTE(task1 + task2) \sim Condition + (1|Subject)$ with the BF of individual model as $PTE(task1) \sim Condition + (1|Subject)$, where *task1* denotes the Treasure Hunt (original) task and *task2* denotes the Water Maze (replication) task. We calculated the ratio $BF(task1 + task2)/BF(task1)$, which was used to quantify the degree of replicability. We determined whether the degree of replicability was higher than 3 as BF of at least 3 indicates evidence for replicability (Jeffreys 1998). A BF of at least 100 is considered as "*decisive*" for degree of replication (Jeffreys 1998).

We used similar BF analysis methods to estimate the degree of replicability for the direction of information flow across spatial and verbal episodic memory domains (see Das and Menon 2021, for results pertaining to the verbal episodic memory task). The frequency range of broadband in the verbal episodic and spatial memory tasks was different; hence, the BF analysis was carried out for the delta–theta and beta-frequency bands for determining replicability across verbal episodic and spatial memory domains. We compared the BF of the joint model $PTE(task1 + task2 + task3) \sim Condition + (1|Subject)$ for the spatial (replication) and verbal (original) tasks with the BF of the verbal model as $PTE(task3) \sim Condition + (1|Subject)$, where *task3* denotes the verbal episodic memory task. The ratio $BF(task1 + task2 + task3)/BF(task3)$ was used to quantify the degree of replicability across spatial and verbal episodic memory domains.

3. Results

3.1 Treasure Hunt task: causal information flow from the hippocampus on the PFC during successful spatial memory encoding

We first examined the causal dynamic influences of the hippocampus on the middle frontal gyrus (MFG) and inferior frontal gyrus (IFG) nodes of the PFC during the memory encoding period of a Treasure Hunt spatial navigation task (Materials and methods, Supplementary Tables 1, 2a, and 3a, Figs 1a and 2a). Briefly, patients performed multiple trials of a spatial memory task in a virtual reality environment (Miller et al. 2018; Tsitsiklis et al. 2020), where they played a Treasure Hunt task. In each task trial, subjects explored a rectangular arena on a virtual 3D beach to reach treasure chests that revealed hidden objects, with the aim of encoding the location of each item encountered (Fig. 2a). Each task trial begins with the subject placed on the ground at a randomly selected end of the environment. The subject initiates the trial with a button press and then navigates to a chest using a joystick. Upon arrival at the chest, the chest opens and either reveals an object, which the subject should try to remember, or is empty. The subject remains facing the open chest for 1.5 s ("encoding period") and then the object and chest disappear, which indicates that the subject should navigate to the next chest that has now appeared in the arena. Each trial consists of four chests; two or three (randomly selected) of the chests contain an object, and the others are empty. Each session consists of 40 trials, and in each session, subjects visit a total of 100 full chests and 60 empty chests. They then perform a distractor task, a computerized version of the "shell game," before entering the "recall period." During recall, subjects are cued with each of the trial's objects in a random sequence and asked to recall the location of the object. After the location of each object of the trial is indicated, the feedback stage of each trial begins. Here, subjects are shown their response for each cued object

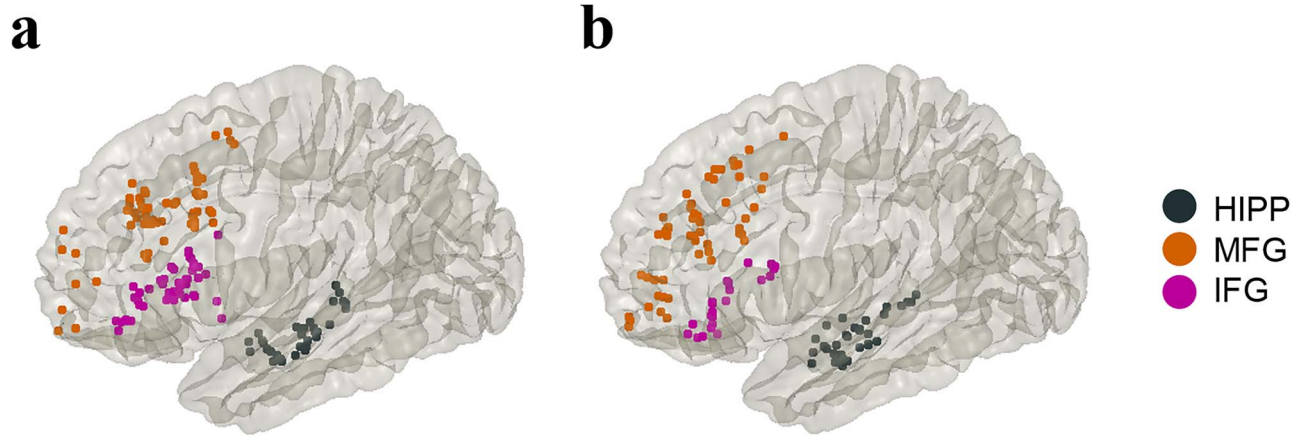

Fig. 1. iEEG recording sites in hippocampus and prefrontal cortex subdivisions investigated during a) Treasure Hunt and b) Water Maze spatial memory tasks. HIPP: Hippocampus, MFG: Middle frontal gyrus, and IFG: Inferior frontal gyrus subdivisions of prefrontal cortex.

in the trial, via a green circle if the location was correct and a red circle if it was incorrect.

We used PTE (Lobier et al. 2014) to compute broadband (0.5–80 Hz) causal influence from the hippocampus to the MFG and IFG in the PFC and vice versa. During successful spatial memory encoding (see Supplementary Figs 1–3 for comparison between successfully and unsuccessfully recalled trials), the hippocampus had greater causal influences on both the MFG ($F(1, 111) = 48.80$, $P < 0.001$) and IFG ($F(1, 150) = 20.66$, $P < 0.001$) nodes than the reverse (Fig. 3a and b, respectively). These results demonstrate that the hippocampus has an asymmetric causal information flow to both the MFG and IFG during successful spatial memory encoding in the Treasure Hunt spatial navigation task.

3.2 Treasure Hunt task: causal information flow from the hippocampus on PFC during successful spatial memory recall

Next, we examined causal influences of the hippocampus on the PFC during the recall phase of the Treasure Hunt spatial memory task, in which participants recalled the location of objects they had seen during the spatial memory encoding phase (Fig. 2a, Materials and methods). During successful spatial memory recall, the hippocampus had higher broadband causal influences on both MFG ($F(1, 112) = 29.02$, $P < 0.001$) and IFG ($F(1, 150) = 7.51$, $P < 0.01$) than the reverse (Fig. 3a and b, respectively).These results demonstrate that the hippocampus has an asymmetric causal information flow to both the MFG and IFG subdivisions of the PFC during successful memory recall in the Treasure Hunt spatial navigation task.

3.3 Treasure Hunt task: differential causal information flow from the hippocampus to MFG and IFG during successful spatial memory encoding and recall

We next examined the differential causal information flow from the hippocampus to the MFG and IFG subdivisions of the PFC based on the hypothesized role of differential involvement of the MFG and IFG in memory processing with the IFG more involved in controlled memory retrieval (Hasegawa et al. 1999; Dobbins et al. 2002). This analysis revealed that the causal influence of the hippocampus on MFG was greater than IFG during successful spatial memory encoding ($F(1, 135) = 25.10$, $P < 0.001$). The causal influence of the MFG and IFG nodes on the hippocampus did not differ from each other during successful spatial memory encoding ($F(1, 132) = 0.95$, $P > 0.05$). Furthermore, the causal influence of the hippocampus on MFG was greater than IFG during successful spatial memory recall ($F(1, 114) = 14.43$, $P < 0.001$). The causal influence of the MFG and IFG nodes on the hippocampus did not differ from each other during successful spatial memory recall ($F(1, 132) = 0.64$, $P > 0.05$).

3.4 Water Maze task: causal information flow from the hippocampus to the PFC during successful spatial memory encoding

Next, we examined dynamic causal influences of the hippocampus on the MFG and IFG nodes of the PFC during the memory encoding period of the Water Maze spatial navigation task (Materials and methods, Supplementary Tables 1, 2b, and 3b, Figs 1b and 2b). Briefly, patients performed multiple trials of a spatial memory task in a virtual navigation paradigm (Jacobs et al. 2016; Goyal et al. 2018; Lee et al. 2018) similar to the Morris Water Maze (Morris 1984) (Fig. 2b). Each trial (96 trials per session, 1–3 sessions per subject) started with two 5-s "encoding periods," during which subjects were driven to an object from a random starting location. At the beginning of an encoding period, the object appeared, and, over the course of 5 s, the subject was automatically driven directly toward it. After a 5-s delay with a blank screen, the same process was repeated from a different starting location. After both encoding periods for each item, there was a 5-s pause followed by the "recall

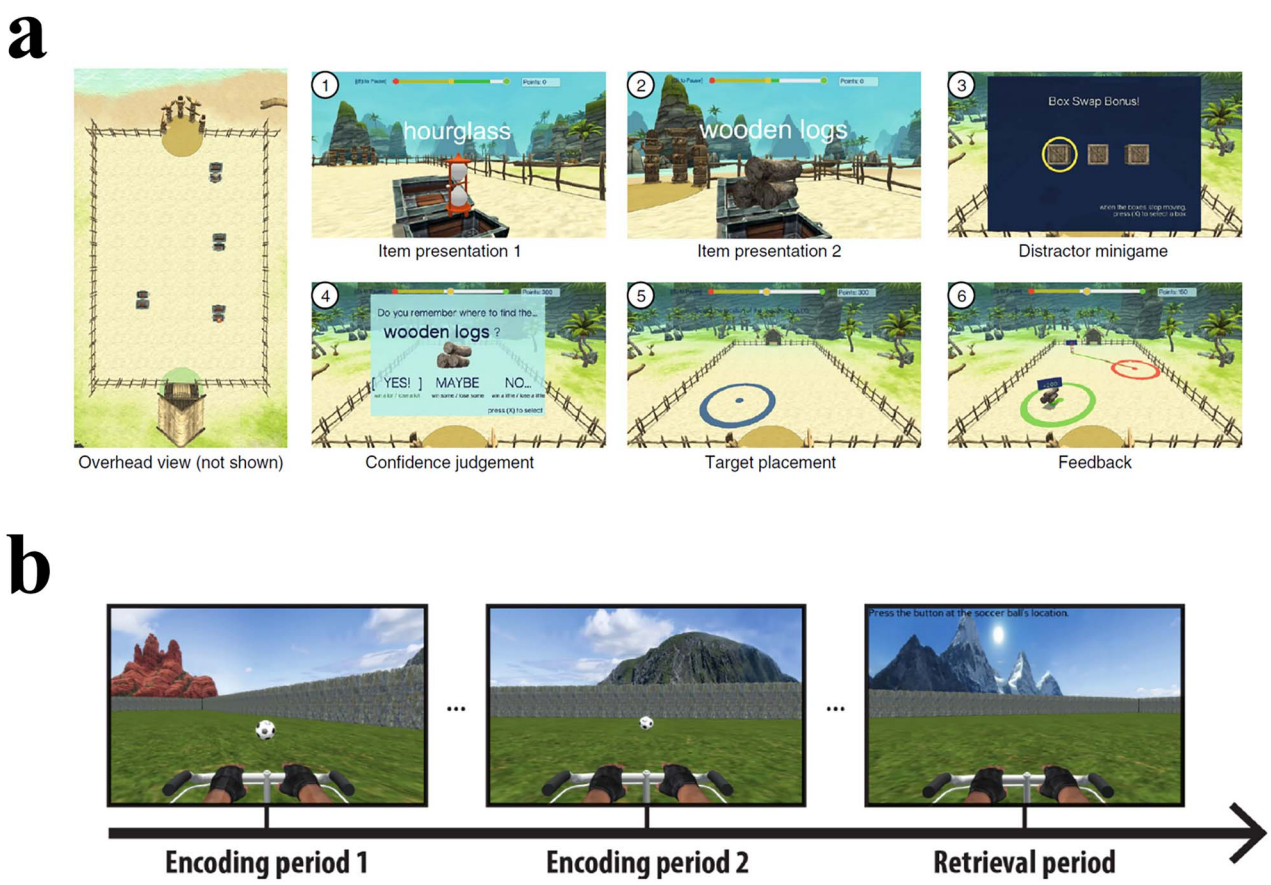

Fig. 2. Event structure of encoding and recall periods of the spatial navigation and memory tasks. a) Treasure Hunt task. The leftmost image shows an overhead view of the virtual reality environment for this task with the chest positions visible. This overhead view is never shown to subjects and only one chest is visible at a time during the task. Panels 1–6 indicate an example sequence of events that subjects encounter during each trial of the task (see Materials and methods for details): (1) first item presentation, (2) second item presentation, (3) the distractor period before the retrieval period, (4) the confidence judgment, (5) response period where subjects indicate an item's remembered location, and (6) feedback. Taken from Miller et al. (2018) with permission. b) Water Maze task. Each trial began with a 2-s stationary wait period during which subjects viewed the virtual reality environment. Each encoding event consisted of two encoding trials of 5 s each, corresponding to two different starting points in the virtual reality environment for each target location. For each encoding trial, once the target object appeared, subjects were automatically rotated toward and then driven to the target location. After the encoding trials, subjects were transported to a new location for the retrieval phase and asked to drive themselves to the target location and respond by pressing a button. Feedback was provided by displaying a map of the target and response location, along with game points that correlated with distance error, similar to the Treasure Hunt task. Taken from Jacobs et al. (2016) with permission.

period." The subject was placed in the environment at a random starting location with the object hidden and then asked to freely navigate using a joystick to the location where they thought the object was located. When they reached their chosen location, they pressed a button to record their response. They then received feedback on their performance via an overhead view of the environment showing the actual and reported object locations.

We repeated our analysis using PTE (Lobier et al. 2014) to compute broadband (0.5–80 Hz) causal influence from the hippocampus to the MFG and IFG in the PFC and vice versa, similar to the Treasure Hunt spatial navigation task. During successful spatial memory encoding, the hippocampus had greater broadband causal influences on both the MFG ($F(1, 95) = 164.05$, $P < 0.001$) and IFG ($F(1, 56) = 62.07$, $P < 0.001$) nodes than the reverse (Fig. 3c and d, respectively). These results demonstrate that the hippocampus has an asymmetric causal information flow to both the MFG and IFG during successful spatial memory encoding in the Water Maze spatial navigation task.

3.5 Water Maze task: causal information flow from the hippocampus on PFC during successful spatial memory recall

Next, we examined causal influences of the hippocampus on the PFC during the recall phase of the Water Maze spatial memory task in which participants recalled the location of objects they had seen during the spatial memory encoding phase (Fig. 2b, Materials and methods). During successful spatial memory recall, the hippocampus had higher broadband causal influences on both MFG ($F(1, 95) = 181.2$, $P < 0.001$) and IFG ($F(1, 56) = 72.37$, $P < 0.001$) than the reverse (Fig. 3c and d, respectively). These results demonstrate that the hippocampus has an asymmetric causal information flow to both the MFG and IFG subdivisions of the PFC during successful spatial memory recall in the Water Maze spatial navigation task.

3.6 Water Maze task: differential causal information flow from the hippocampus to MFG and IFG during successful spatial memory encoding and recall

We examined the differential causal information flow from the hippocampus to the MFG and IFG subdivisions of the PFC during the Water Maze spatial navigation task. This analysis revealed that the causal influence of the hippocampus on IFG was higher than that of MFG during successful spatial memory encoding ($F(1, 68) = 7.03$, $P < 0.01$), a trend exactly opposite to that observed in the Treasure Hunt spatial navigation task. However, the causal influence of the MFG and IFG nodes on the hippocampus did not differ from each other during successful spatial memory encoding ($F(1, 77) = 1.87$, $P > 0.05$). Furthermore, the causal influence of the hippocampus on IFG was higher than that of MFG during successful spatial memory recall ($F(1, 46) = 25.06$, $P < 0.001$), again, a trend exactly opposite to that observed in the Treasure Hunt spatial navigation task. The causal influence of the IFG on the hippocampus was greater than the causal influence of the MFG on the hippocampus during successful spatial memory recall ($F(1, 76) = 16.33$, $P < 0.001$).

3.7 Treasure Hunt task: causal information flow from the hippocampus to the PFC in the delta–theta frequency band

Based on previous findings from iEEG studies that have reported significant delta–theta frequency (0.5–8 Hz) band activity in the hippocampus during spatial information recall from recently encoded memories and hippocampal–PFC interactions during spatial memory recall (Watrous et al. 2013; Ekstrom and Watrous 2014; Neuner et al. 2014), we next investigated the dynamic causal influences of the hippocampus on the PFC nodes and vice versa in the low-frequency delta–theta (0.5–8 Hz) band. We first computed PTE from the PFC nodes to the hippocampus and, in the reverse direction, during successful spatial memory encoding and recall in the delta–theta (0.5–8 Hz) frequency band in the Treasure Hunt spatial navigation task. This analysis revealed that the hippocampus has higher causal influences on the MFG and IFG subdivisions of the PFC than the reverse during both the successful spatial memory encoding ($F(1, 111) = 117.45$, $P < 0.001$ for MFG and $F(1, 149) = 34.33$, $P < 0.001$ for IFG) and recall ($F(1, 111) = 69.26$, $P < 0.001$ for MFG and $F(1, 149) = 45.76$, $P < 0.001$ for IFG) conditions (Fig. 4a and b). These results demonstrate a key role for delta–theta frequency signaling underlying higher causal influences of the hippocampus on the PFC in the Treasure Hunt spatial navigation task.

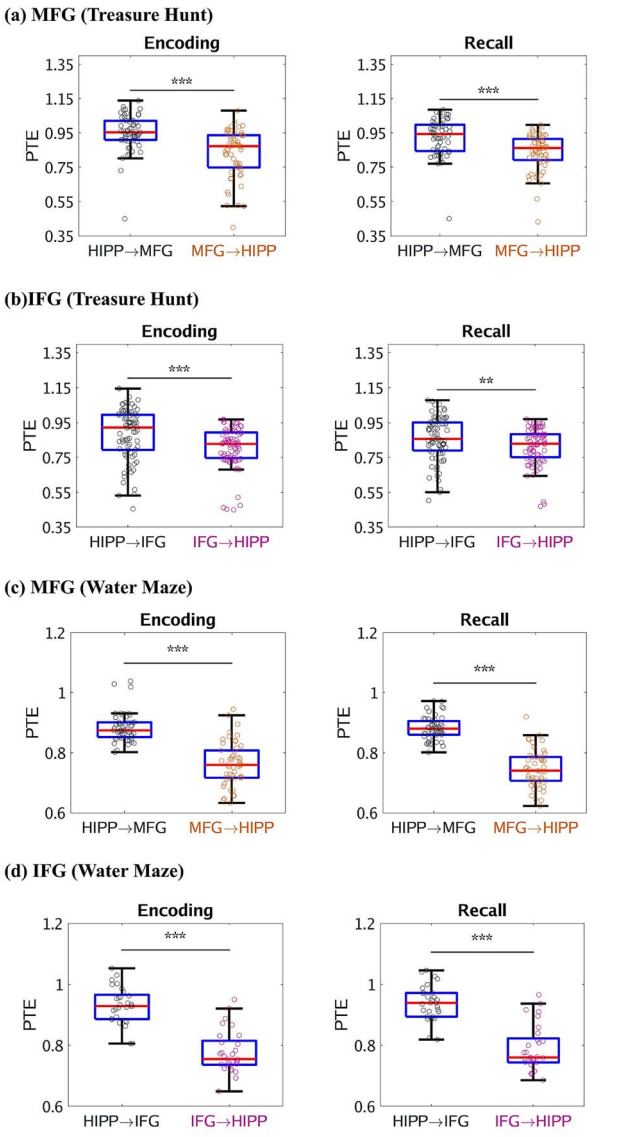

Fig. 3. Causal directed information flow between hippocampus and prefrontal cortex during Treasure Hunt and Water Maze spatial navigation tasks, measured using PTE. Treasure Hunt: a) the hippocampus showed higher causal directed information flow to the MFG (HIPP → MFG) during memory encoding and recall, compared with the reverse direction (MFG → HIPP) ($n = 59$). b) The hippocampus also showed higher causal directed information flow to the IFG (HIPP → IFG) during memory encoding and recall, than the reverse direction (IFG → HIPP) ($n = 78$). Water Maze: c) the hippocampus showed higher causal directed information flow to the MFG (HIPP → MFG) during memory encoding and recall, compared with the reverse direction (MFG → HIPP) ($n = 50$). d) The hippocampus also showed higher causal directed information flow to the IFG (HIPP → IFG) during memory encoding and recall, than the reverse direction (IFG → HIPP) ($n = 29$). Only trials corresponding to successful memory recall are considered. On each box, the central mark indicates the median, and the bottom and top edges of the box indicate the 25th and 75th percentiles, respectively. Whiskers extend to the most extreme data points not considered outliers. *** $P < 0.001$, ** $P < 0.01$ (two-way ANOVA, FDR-corrected).

3.8 Water Maze task: causal information flow from the hippocampus to the PFC in the delta–theta frequency band

Next, we repeated our PTE analysis and estimated causal information flow from the PFC nodes to the hippocampus and, in the reverse direction, during successful spatial memory encoding and recall in the delta–theta (0.5–8 Hz) frequency band in the Water Maze spatial navigation task. Similar to the Treasure Hunt spatial navigation task, this analysis revealed that the hippocampus has higher causal influences on the MFG

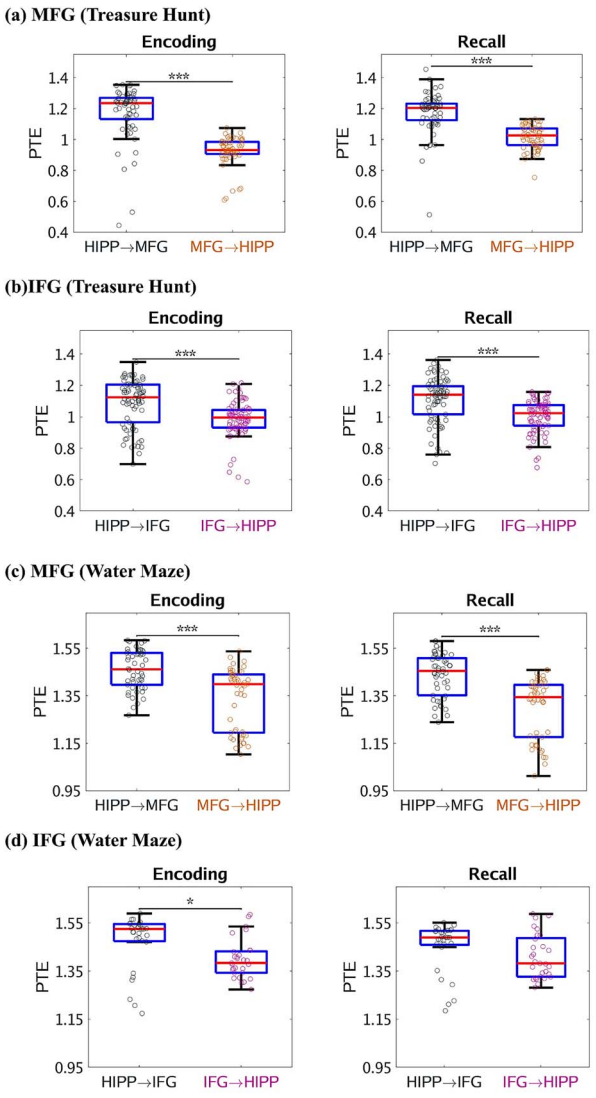

Fig. 4. Causal directed information flow from hippocampus to prefrontal cortex during Treasure Hunt and Water Maze spatial navigation tasks in the delta–theta (0.5–8 Hz) frequency band. Treasure Hunt: a) causal directed information flow from hippocampus to MFG (HIPP → MFG) was greater during both memory encoding and recall, compared with the reverse direction (MFG → HIPP) ($n = 59$). b) Similarly, causal directed information flow from hippocampus to IFG (HIPP → IFG) was greater during both memory encoding and recall, compared with the reverse direction (IFG → HIPP) ($n = 78$). Water Maze: c) causal directed information flow from hippocampus to MFG (HIPP → MFG) was greater during both memory encoding and recall, compared with the reverse direction (MFG → HIPP) ($n = 50$). d) Causal directed information flow from hippocampus to IFG (HIPP → IFG) was greater during memory encoding, compared with the reverse direction (IFG → HIPP) ($n = 29$). Only trials corresponding to successful memory recall are considered. On each box, the central mark indicates the median, and the bottom and top edges of the box indicate the 25th and 75th percentiles, respectively. Whiskers extend to the most extreme data points not considered outliers. *** $P < 0.001$, * $P < 0.05$ (two-way ANOVA, FDR-corrected).

and IFG subdivisions of the PFC than the reverse during successful spatial memory encoding and recall in all except one conditions ($F(1, 95) = 127.61$, $P < 0.001$ for MFG and $F(1, 56) = 10.04$, $P < 0.05$ for IFG during encoding; $F(1, 95) = 214.67$, $P < 0.001$ for MFG and $F(1, 56) = 2.92$, $P > 0.05$ for IFG during recall) (Fig. 4c and d). Replication of the same results in the delta–theta frequency band during the Water Maze spatial navigation task emphasizes a key role for delta–theta frequency signaling underlying higher causal influences of the hippocampus on the PFC.

3.9 Treasure Hunt task: causal information from the PFC to the hippocampus in the beta-frequency band

Next, we examined frequency-specific information flow between the hippocampus and PFC based on emerging findings in nonhuman primates regarding cortical signaling in the beta-frequency (12–30 Hz) band during cognition (Engel and Fries 2010). We computed PTE from the PFC nodes to the hippocampus, and in the reverse direction, during successful spatial memory encoding, and recall in the beta-frequency (12–30 Hz) band in the Treasure Hunt spatial navigation task. Surprisingly, this analysis revealed that the MFG and IFG nodes of the PFC had greater causal influences on the hippocampus during both successful spatial memory encoding ($F(1, 112) = 48.45$, $P < 0.001$ for MFG and $F(1, 150) = 164.59$, $P < 0.001$ for IFG) and recall ($F(1, 113) = 57.56$, $P < 0.001$ for MFG and $F(1, 150) = 87.08$, $P < 0.001$ for IFG) conditions (Fig. 5a and b). These results demonstrate a key role for beta-frequency signaling underlying higher causal influences of the PFC on the hippocampus.

3.10 Water Maze task: causal information from the PFC to the hippocampus in the beta-frequency band

We next repeated our PTE analysis and estimated the directed causal information flow between the PFC and the hippocampus, during successful spatial memory encoding, and recall in the beta-frequency (12–30 Hz) band in the Water Maze spatial navigation task. Similar to the Treasure Hunt spatial navigation task, this analysis revealed that the MFG and IFG nodes of the PFC had higher causal influences on the hippocampus during both successful spatial memory encoding ($F(1, 98) = 32.15$, $P < 0.001$ for MFG and $F(1, 56) = 68.16$, $P < 0.001$ for IFG) and recall ($F(1, 95) = 34.66$, $P < 0.001$ for MFG and $F(1, 56) = 69.67$, $P < 0.001$ for IFG) conditions (Fig. 5c and d). Replication of same results in the beta-frequency band during the Water Maze spatial navigation task recapitulate a key role for beta-frequency signaling underlying higher causal influences of the PFC on the hippocampus.

3.11 Treasure Hunt and Water Maze tasks: replication of findings within the spatial memory domain

We used replication BF (Verhagen and Wagenmakers 2014; Ly et al. 2019) analysis to estimate the degree of replicability for the direction of information flow for each frequency and task condition and across the two spatial memory tasks (Table 1). We used the posterior distribution obtained from the Treasure Hunt (original) data as a prior distribution for the test of data from the Water Maze (replication) dataset (Ly et al. 2019) (Materials and methods).

Table 1. Replicability of findings across Treasure Hunt and Water Maze spatial memory tasks. a) Memory encoding and b) memory recall. The Treasure Hunt task was considered the original dataset, and the Water Maze task was considered the replication dataset.

a) Memory encoding

Finding	Frequency band	Bayes factor for replication
HIPP → MFG > MFG → HIPP	Broadband (0.5–80 Hz)	1.19e+19
HIPP → MFG > MFG → HIPP	Delta–theta (0.5–8 Hz)	1.13e+24
MFG → HIPP > HIPP → MFG	Beta (12–30 Hz)	1.73e+4
HIPP → IFG > IFG → HIPP	Broadband (0.5–80 Hz)	3.81e+4
HIPP → IFG > IFG → HIPP	Delta–theta (0.5–8 Hz)	7.26e−1
IFG → HIPP > HIPP → IFG	Beta (12–30 Hz)	1.51e+10

b) Memory recall

Finding	Frequency band	Bayes factor for replication
HIPP → MFG > MFG → HIPP	Broadband (0.5–80 Hz)	2.24e+16
HIPP → MFG > MFG → HIPP	Delta–theta (0.5–8 Hz)	1.97e+29
MFG → HIPP > HIPP → MFG	Beta (12–30 Hz)	1.97e+29
HIPP → IFG > IFG → HIPP	Broadband (0.5–80 Hz)	5.46e+3
HIPP → IFG > IFG → HIPP	Delta–theta (0.5–8 Hz)	3.06e−4
IFG → HIPP > HIPP → IFG	Beta (12–30 Hz)	1.32e+8

We first used the replication BF analysis for the memory encoding periods of the two spatial tasks (Table 1a). Findings corresponding to the direction of information flow between hippocampus and MFG during memory encoding were replicated in broadband, delta–theta band, and beta band (BFs 1.19e+19, 1.13e+24, and 1.73e+4, respectively). Findings corresponding to the direction of information flow between hippocampus and IFG during memory encoding were replicated in broadband and beta band (BFs 3.81e+4 and 1.51e+10, respectively), but not in delta–theta band (BF 7.26e−1).

We next repeated the replication BF analysis for the memory recall periods of the two spatial tasks (Table 1b). Findings corresponding to the direction of information flow between hippocampus and MFG during memory recall were replicated in broadband, delta–theta band, and beta band (BFs 2.24e+16, 1.97e+29, and 1.97e+29, respectively). Findings corresponding to the direction of information flow between hippocampus and IFG during memory recall were replicated in broadband and beta band (BFs 5.46e+3 and 1.32e+8, respectively), but not in delta–theta band (BF 3.06e−4). Together, these results demonstrate very high replicability of direction of information flow between hippocampus and PFC across the two spatial memory tasks and also indicate that findings corresponding to the direction of information flow between the hippocampus and MFG are more replicable than those corresponding to the direction of information flow between hippocampus and IFG.

We also found that the hippocampus → MFG versus hippocampus → IFG findings had BF of 1.19e−2 and 5.15e−3 for memory encoding and recall, respectively, indicating that differential information flow from the hippocampus to the MFG and IFG is not replicable across spatial tasks. Furthermore, MFG → hippocampus versus IFG → hippocampus findings had BF of 9.76e+1 and 4.02e+3 for memory encoding and recall, respectively, indicating that differential information flow from the MFG and IFG to the hippocampus is replicable across spatial tasks; however, the BFs are relatively low compared with BFs in Tables 1 and 2.

3.12 Replication of findings across spatial and verbal memory domains

We repeated the replication BF analysis to estimate the degree of replicability of direction of information flow across spatial and nonspatial domains (Table 2). Specifically, we estimated the degree of replicability between the verbal episodic memory (original) task used in our previous study (Das and Menon 2021) and the two spatial navigation tasks (replication) used in the present study. Similar to above analysis, we used the posterior distribution obtained from the verbal episodic memory (original) dataset as a prior distribution for the test of data from the spatial memory (replication) tasks (Ly et al. 2019) (Materials and methods). The frequency range of broadband in the verbal episodic and spatial memory tasks was different; hence, the replication BF analysis was carried out for the delta–theta and beta-frequency bands for determining replicability across verbal episodic and spatial memory tasks.

We first used replication BF analysis for the memory encoding periods of the verbal episodic and spatial memory tasks (Table 2a). Findings corresponding to the direction of information flow between hippocampus and MFG during memory encoding were replicated in both delta–theta and beta bands (BFs 8.51e+35 and 1.26e+12, respectively). Findings corresponding to the direction of information flow between hippocampus and IFG during memory encoding were also replicated in both delta–theta and beta bands (BFs 7.32e+8 and 9.36e+28, respectively).

We next repeated the replication BF analysis for the memory recall periods of the verbal episodic and spatial memory tasks (Table 2b). Findings corresponding to the direction of information flow between hippocampus

Table 2. Replicability of findings across verbal episodic and spatial memory tasks. a) Memory encoding and b) memory recall. The frequency range of broadband in the verbal episodic and spatial memory tasks were different; hence, the Bayes factor analysis was carried out for the delta–theta and beta-frequency bands for determining replicability across verbal episodic and spatial memory tasks. The verbal episodic memory task was considered the original dataset and the spatial tasks were considered the replication dataset.

a) Memory encoding

Finding	Frequency	Bayes factor for replication
HIPP → MFG > MFG → HIPP	Delta–theta (0.5–8 Hz)	8.51e+35
MFG → HIPP > HIPP → MFG	Beta (12–30 Hz)	1.26e+12
HIPP → IFG > IFG → HIPP	Delta–theta (0.5–8 Hz)	7.32e+8
IFG → HIPP > HIPP → IFG	Beta (12–30 Hz)	9.36e+28

b) Memory recall

Finding	Frequency	Bayes factor for replication
HIPP → MFG > MFG → HIPP	Delta–theta (0.5–8 Hz)	8.62e+33
MFG → HIPP > HIPP → MFG	Beta (12–30 Hz)	8.12e+8
HIPP → IFG > IFG → HIPP	Delta–theta (0.5–8 Hz)	1.44e+11
IFG → HIPP > HIPP → IFG	Beta (12–30 Hz)	2.91e+19

and MFG during memory recall were replicated in both delta–theta and beta bands (BFs 8.62e+33 and 8.12e+8, respectively). Findings corresponding to the direction of information flow between hippocampus and IFG during memory recall were also replicated in both delta–theta and beta bands (BFs 1.44e+11 and 2.91e+19, respectively). Together, these results demonstrate very high replicability of direction of information flow between hippocampus and PFC across spatial and nonspatial domains.

3.13 Treasure Hunt and Water Maze tasks: surrogate data analysis of causal information flow between the hippocampus and the PFC

Next, we conducted surrogate data analysis to test the significance of the estimated PTE values compared with PTE expected by chance (Materials and methods). The estimated phases from the Hilbert transform for electrodes from pairs of brain areas were time-shuffled, and PTE analysis was repeated on this shuffled data to build a distribution of surrogate PTE values against which the observed PTE was tested. This analysis revealed that causal information flow from the hippocampus to both the MFG and IFG was significantly higher than those expected by chance in broadband during both successful spatial memory encoding and recall conditions and across spatial navigation tasks ($Ps < 0.05$).

Frequency-specific surrogate data analysis further revealed that causal information flow from the hippocampus to the MFG and IFG nodes of the PFC and the reverse was significantly higher than that expected by chance ($P < 0.05$ in all cases) in the delta–theta frequency band for both successful memory encoding and recall and across spatial navigation tasks, indicating bidirectional causal information flow between the hippocampus and the PFC in delta–theta band. Analysis in the beta-frequency band revealed that causal information flow from the hippocampus to the MFG and IFG and the reverse was significantly lower than that expected by chance ($P < 0.05$ in all cases) for both successful memory encoding and recall and across spatial navigation tasks, indicating significantly lower predictability of one brain area from the other than expected by chance, in this frequency band.

These results demonstrate that the reported effects in this study arise from causal signaling that is significantly enhanced above chance levels.

3.14 Treasure Hunt and Water Maze tasks: power spectral density during spatial memory encoding and recall across multiple spatial navigation tasks

Finally, we compared the power spectral density (Materials and methods, Supplementary Table 3) in the hippocampus and the MFG and IFG nodes of the PFC across spatial memory encoding and recall conditions. This analysis revealed that the power in the two conditions does not differ from each other in any region (hippocampus/MFG/IFG) and in any of the two spatial navigation tasks (all $Ps > 0.05$).

Previous studies have suggested that power in the high gamma band (80–160 Hz) is correlated with fMRI BOLD signals (Leopold et al. 2003; Mantini et al. 2007; Scholvinck et al. 2010; Hutchison et al. 2015; Lakatos et al. 2019) and is thought to reflect local activity (Canolty and Knight 2010). We compared high-gamma-band power spectral density (see Materials and methods for details) in the hippocampus and the MFG and IFG across spatial memory encoding and recall conditions in both the spatial navigation tasks. This analysis revealed that the power under the two conditions did not differ from each other in any of the three regions and in any of the two spatial navigation tasks (all $Ps > 0.05$).

4. Discussion

We examined directed information flow between the hippocampus and distinct PFC subdivisions during performance of two different spatial navigation tasks in which participants were asked to memorize object locations

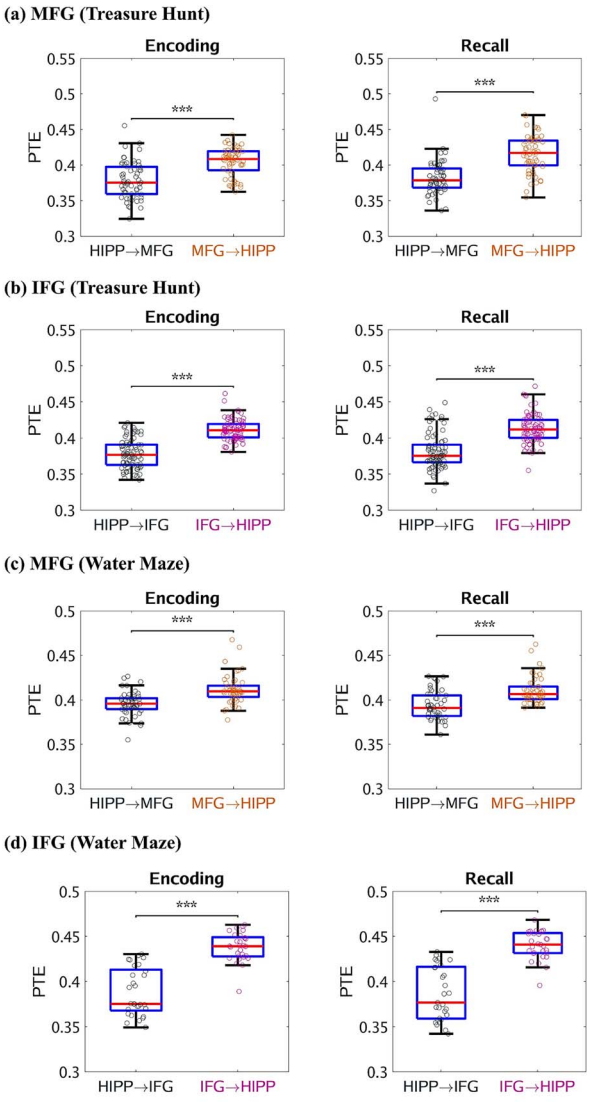

Fig. 5. Causal directed information flow between hippocampus and prefrontal cortex during Treasure Hunt and Water Maze spatial navigation tasks in the beta (12–30 Hz) frequency band. Treasure Hunt: a) hippocampus → MFG (HIPP → MFG) during memory encoding and recall ($n = 59$). b) Hippocampus → IFG (HIPP → IFG) during memory encoding and recall ($n = 78$). Both MFG and IFG nodes had higher causal influences on the hippocampus than the reverse during both memory encoding and recall in the beta-frequency band. Water Maze: c) hippocampus → MFG (HIPP → MFG) during memory encoding and recall ($n = 50$). d) Hippocampus → IFG (HIPP → IFG) during memory encoding and recall ($n = 29$). Both MFG and IFG nodes had higher causal influences on the hippocampus than the reverse during both memory encoding and recall in the beta-frequency band. Only trials corresponding to successful memory recall are considered. On each box, the central mark indicates the median, and the bottom and top edges of the box indicate the 25th and 75th percentiles, respectively. Whiskers extend to the most extreme data points not considered outliers. *** $P < 0.001$ (two-way ANOVA, FDR-corrected).

by navigating in a virtual spatial environment and later asked to recall the locations of the objects (Solomon et al. 2019). Both tasks consisted of multiple trials involving memory encoding and recall. We leveraged a unique sample of iEEG recordings from the UPENN-RAM cohort that included data from 40 participants, 248 electrodes, and 216 electrode pairs. Direction-specific information theoretic analysis revealed that the hippocampus has a greater causal influence on both the MFG and IFG subdivisions of the PFC than the reverse, and crucially, this pattern was observed during both the spatial memory encoding and recall phases, and across multiple spatial navigation tasks.

In the delta–theta and beta-frequency bands, our analysis revealed frequency specificity of hippocampus–PFC interactions as well as a dissociation between feedforward and feedback information flow from, and to, the hippocampus. During both spatial memory encoding and recall, causal feedforward influences from the hippocampus to the PFC in the delta–theta frequency band were greater than the reverse direction. In contrast, in the beta-frequency band, top-down causal influences from the PFC to the hippocampus were greater than in the reverse direction during both spatial memory encoding and recall. Surrogate data analysis revealed that the strength of information flow between the hippocampus and the PFC was significantly beyond chance levels. Crucially, this frequency specificity of the direction of information flow between the hippocampus and the PFC was detected in both the Treasure Hunt and Water Maze spatial navigation tasks, with a high replicability BF, demonstrating the robustness of our findings. Our findings provide novel insights into the asymmetric directionality of information flow between the hippocampus and the PFC during spatial navigation and memory in the human brain and, for the first time, provide evidence for replicable findings both within the domain of spatial navigation (Table 1) and across spatial and verbal episodic memory domains (Table 2).

4.1 Directionality of information flow between the hippocampus and the PFC during spatial memory processing

The first goal of our study was to characterize the directionality of information flow between the hippocampus and the PFC during spatial memory processing. Although multiple lesion studies in humans have demonstrated the role of the right hemisphere hippocampus in spatial memory formation (Smith and Milner 1989; Abrahams et al. 1997; Spiers et al. 2001; Burgess et al. 2002), the role of the left hemisphere in spatial memory is less clear, with several lesion studies pointing to the involvement of both the left and right hemisphere hippocampus in spatial memory (Maguire et al. 1996; Bohbot et al. 1998; Spiers et al. 2001). Moreover, the role of directed causal information flow between the left hemisphere hippocampus and the PFC in spatial navigation and memory remains unclear as fMRI, the mainstay of hippocampus–PFC investigations in humans, lacks the required temporal resolution to investigate causal circuit dynamics.

Building on our previous work on the direction of causal information flow between the left hemisphere hippocampus and the PFC in verbal episodic memory encoding and recall (Das and Menon 2021), here we

focused on the left hemisphere hippocampus interactions with MFG and IFG subdivisions of the PFC. PTE provides a robust and powerful tool to characterize information flow between brain regions based on phase coupling (Lobier et al. 2014; Hillebrand et al. 2016; Wang et al. 2017); unlike phase locking or coherence measures, PTE probes causal influences and determines how one region drives another (Das and Menon 2020). PTE revealed significantly higher broadband causal influence of the hippocampal electrodes on the MFG and IFG electrodes than the reverse during both successful encoding and spatial memory recall. Crucially, this asymmetric pattern of directed causal information flow was replicated in multiple virtual spatial navigation tasks. Both tasks were conceptually similar, consisting of multiple trials of encoding and recall periods. We analyzed trials corresponding to successful memory encoding and recall, from the point of view of probing behaviorally effective memory encoding, our focus was therefore on successful recall consistent with most prior studies (Watrous et al. 2013; Long et al. 2014). These findings converge on recent findings from iEEG recordings in humans in virtual (Miller et al. 2018) as well as real-world (Stangl et al. 2021) spatial navigation tasks that have shown that the left hippocampus plays a crucial role in spatial memory encoding. The findings are also consistent with previous multiple structural and functional MRI (Maguire et al. 1999, 2000; Grön et al. 2000; Iglói et al. 2010; Kaplan et al. 2014), positron imaging tomography (Ghaem et al. 1997; Maguire et al. 1998, 1999), and magnetoencephalography (MEG) (Pu et al. 2017) studies in humans that have revealed the involvement of bilateral hippocampus in spatial navigation and memory. Thus, our findings provide robust electrophysiological evidence for the dynamic causal influence of the left hippocampus on both the MFG and IFG subdivisions of the PFC during both spatial memory encoding and recall. The UPENN-RAM data did not contain enough electrodes simultaneously in the right hemisphere hippocampus and PFC. Further iEEG studies using bilateral recordings will be needed to investigate hemispheric differences in hippocampus–PFC dynamic causal interactions and differences between spatial and verbal domains.

4.2 Frequency-specific directionality of information flow between the hippocampus and the PFC

The second goal of our study was to investigate the frequency specificity of the directional information flow between the hippocampus and the PFC in spatial memory. Based on previous reports in rodents, nonhuman primates, and humans, we focused on delta–theta (0.5–8 Hz) and beta (12–30 Hz) frequency bands, as enhanced local field potentials in these frequency bands have been identified in the hippocampus and PFC, respectively (Engel and Fries 2010; Watrous et al. 2013; Ekstrom and Watrous 2014; Stanley et al. 2018). Previous iEEG studies have reported significant delta–theta frequency (0.5–8 Hz) band activity in the hippocampus during recall of spatial information from recently encoded memories (Jacobs et al. 2016; Goyal et al. 2018), but the frequency specificity of causal hippocampal–PFC signaling in the human brain associated with spatial memory encoding and recall has not been well understood. Our analysis revealed two key dissociations in the frequency-specific directionality of information flow between the hippocampus and PFC.

In the delta–theta band, we found that the hippocampus had higher causal influences on the PFC, compared with the reverse direction; this pattern was observed during both spatial memory encoding and recall periods and in multiple spatial navigation tasks. This finding is consistent with reports of delta–theta frequency band hippocampal–PFC synchronization during spatial memory recall (Watrous et al. 2013; Ekstrom and Watrous 2014) and extends previous reports in fMRI that point to the involvement of the left PFC in spatial memory processing (Burgess et al. 2001; Spiers and Maguire 2006; Kaplan et al. 2012; Epstein et al. 2017; Javadi et al. 2017), by demonstrating directed causal influences from the hippocampus to PFC during the same. In contrast, we found an opposite pattern in the beta band with higher causal influences of PFC on the hippocampus, compared with the reverse direction; again, this pattern was observed during both memory encoding and recall periods and in multiple spatial navigation tasks.

Top-down information flow from the PFC in the beta band may contribute to the transition and maintenance of latent neuronal ensembles into “active” representations (Engel and Fries 2010; Spitzer and Haegens 2017), similar to findings reported with verbal memory encoding and recall (Das and Menon 2021). Our findings inform theoretical models that have argued for frequency specificity of direction of information flow in the human brain across multiple cognitive domains. Higher directed causal outflow from the PFC to the temporal lobe has been observed in MEG recordings in the beta-frequency band during a language processing task involving reading sentences (Schoffelen et al. 2017). Top-down directed information flow in the beta-frequency band has also been hypothesized to be involved in information processing in the human auditory cortex in iEEG recordings where participants passively listened to spoken sentences (Fontolan et al. 2014). In contrast, delta–theta rhythms in the hippocampus may signal pattern completion associated with memory recall that is conveyed to multiple PFC regions (Eichenbaum 2017).

Our findings also converge on spatial encoding and retrieval dynamics reported in rodents. Coherence between the hippocampus and the PFC is a prominent mechanism that helps in spatial encoding and retrieval in rodents (Jones and Wilson 2005; Benchenane et al. 2010). It has been hypothesized, but not directly tested as in our study, that this coherence may allow flow of information from the hippocampus about the animal’s

position or trajectory to trigger place-related associations in downstream regions such as the prefrontal cortex. Outflow of information from the hippocampus is also associated with efficient spatial memory encoding and learning in awake rodents (Kim et al. 2012; Tang et al. 2017) and monkeys (Wirth et al. 2003). Our findings provide evidence for a causal feedback loop between the hippocampus and the PFC, which may help in information replay and support memory formation. Taken together, our findings pertaining to frequency-specific directed causal interactions between the hippocampus and the PFC provide robust evidence that the PFC and hippocampus have different preferential frequencies to create a feedback loop and parallel channels of communication in the human brain to achieve memory encoding and retrieval of spatial information.

The behavioral role of directional connectivity is currently unknown. Previous iEEG studies in humans (Watrous et al. 2013; Ekstrom and Watrous 2014) have not examined directed information flow between the hippocampus and the PFC. In a study of associative learning in nonhuman primates, Brincat and Miller 2015 reported higher causal bottom-up influence from the hippocampus to the PFC in the beta-frequency band for correct compared with the incorrect trials. However, most previous studies in humans have typically reported stronger top-down, rather than bottom-up, causal signaling from the PFC in the beta band (Fontolan et al. 2014; Schoffelen et al. 2017; Das and Menon 2021). Therefore, the broader functional implications and replicability of findings from the Brincat and Miller (2015) study are not clear. We did not find such an effect in any of the three datasets we examined. Increased coherence and directional connectivity between the hippocampus and PFC has been most consistently associated with increased attention and stimulus saliency (Eichenbaum 2017; Ekstrom et al. 2017; Herweg and Kahana 2018; Rutishauser et al. 2021). In the present study, it is not clear how memory recall errors may be related to these factors. Moreover, it is possible that directed connectivity is more closely related to vividness and confidence of recall rather than accuracy (Hebscher et al. 2019). At the present time, the contributions of these factors to causal signaling between the hippocampus and PFC remain an unresolved issue, and further studies with denser sampling of electrodes simultaneously in the hippocampus and the PFC with confidence and vividness ratings (Hebscher and Gilboa 2016) are required to address this question. An alternate possibility is that memory effects with respect to correct and incorrect recall may depend on other hippocampal circuits including the posterior cingulate cortex (Barack and Platt 2021).

4.3 PTE, rather than power spectral density, underlies causal information flow

PTE, as used in the present study, provides a robust measure of the direction of information flow between electrode pairs (Lobier et al. 2014; Hillebrand et al. 2016). Previous findings using multielectrode array recordings in both humans and animal models have established that phase, rather than amplitude, is crucial for both spatial and temporal encoding of information in the brain (Lachaux et al. 1999; Kayser et al. 2009; Siegel et al. 2009; Lopour et al. 2013; Ng et al. 2013). Consistent with this, we found no differences in overall power across memory encoding and recall conditions and across multiple spatial navigation tasks in any of the three regions of the brain examined here: the hippocampus, MFG, and IFG. Taken together, these results suggest that phase, rather than power spectral density, underlies the causal information flow reported here.

4.4 Replication of findings across multiple spatial navigation tasks, and spatial, verbal domains

The third major goal of our study was to replicate findings across tasks and stimulus domains. Replication of findings is a major problem in neuroscience, especially in iEEG studies where data sharing is virtually nonexistent and data are difficult to acquire across multiple brain regions. We used left hemisphere recordings to probe information flow between the hippocampus and the PFC and determine commonalties across spatial and verbal domains. Recent studies using fMRI have pointed to the involvement of both the left and right hemisphere hippocampus and PFC for spatial memory processing; however, the role of left hemisphere hippocampal–PFC interactions for spatial memory recall remains controversial.

We used replication BF (Verhagen and Wagenmakers 2014; Ly et al. 2019) analysis to estimate the degree of replicability for the direction of information flow for each frequency and task condition and across the two spatial memory tasks (Table 1). A recent study (Scheuble and Beauducel 2020) of event-related potentials during deception about attitudes using scalp EEG data replicated its findings across multiple scalp EEG datasets and reported very high replication BF. Very high replication BFs in all our findings except two (Table 1) emphasize the robustness of our findings, which is very challenging in iEEG research. Moreover, we found that BFs associated with the replication of direction of information flow between the hippocampus and the MFG were decisive compared with that associated with the replication of information flow between the hippocampus and the IFG where all except two were decisive. This indicates relatively higher robust replication of information flow associated with the MFG compared with that associated with the IFG across the two spatial memory tasks.

We then repeated our replication BF analysis to estimate the degree of replicability between verbal episodic memory tasks used in our previous study (Das and Menon 2021) and the two spatial navigation tasks used in the present study. We used results from the verbal domain as the original study and results from the Treasure Hunt and Water Maze tasks as the replication

study. Again, we found very high replication BF indicating high degree of replicability across the spatial and verbal domains (Table 2). Our findings provide novel insights into the asymmetric directionality of information flow between left hemisphere hippocampus and PFC during spatial navigation and memory in the human brain and, for the first time, provide evidence for replicable findings both within the domain of spatial navigation and memory formation and across spatial and nonspatial domains (Das and Menon 2021). These findings reveal common domain-independent casual signaling mechanisms in human hippocampus–PFC circuits.

5. Conclusions

Our study advances knowledge of directed information flow between the hippocampus and PFC during spatial memory processing in humans. Across two different spatial navigation tasks, we discovered distinct feedforward and feedback signaling mechanisms between the hippocampus and PFC. Findings demonstrate for the first-time separate frequency-specific, orthogonal, channels of communication between hippocampal and prefrontal circuits as well as their association with task performance in humans during virtual environment tasks. Together these findings provide insights into how specific neural signals may differentially contribute to integration of allocentric cues in the spatial environment and cognitive control signals from the PFC. Altering feedforward and feedback signals could help with disorders such as Alzheimer's disease in which spatial navigation is known to be impaired (Coughlan et al. 2018).

Acknowledgments

We are grateful to members of the UPENN-RAM consortia for generously sharing their unique iEEG data. We thank Drs Paul A. Wanda, Michael V. DePalatis, Youssef Ezzyat, Richard Betzel, and Leon A. Davis for assistance with the UPENN-RAM dataset. We thank Drs Matteo Fraschini and Arjan Hillebrand for generously sharing their MATLAB code for PTE analysis. We also thank two anonymous reviewers for providing thoughtful feedback on our manuscript.

Supplementary material

Supplementary material is available at *Cerebral Cortex Journal* online.

Funding

This research was supported by National Institutes of Health grants NS086085, MH126518, and EB022907.

Conflict of interest statement. The authors declare no competing financial interests.

References

Abrahams S, Pickering A, Polkey CE, Morris RG. Spatial memory deficits in patients with unilateral damage to the right hippocampal formation. *Neuropsychologia*. 1997:35(1):11–24. https://doi.org/10.1016/s0028-3932(96)00051-6.

Badre D, Wagner AD. Left ventrolateral prefrontal cortex and the cognitive control of memory. *Neuropsychologia*. 2007:45(13):2883–2901. https://doi.org/10.1016/j.neuropsychologia.2007.06.015.

Badre D, Poldrack RA, Paré-Blagoev EJ, Insler RZ, Wagner AD. Dissociable controlled retrieval and generalized selection mechanisms in ventrolateral prefrontal cortex. *Neuron*. 2005:47(6):907–918. https://doi.org/10.1016/j.neuron.2005.07.023.

Barack DL, Platt ML. Neuronal activity in the posterior cingulate cortex signals environmental information and predicts Behavioral variability during Trapline foraging. *J Neurosci*. 2021:41(12):2703–2712. https://doi.org/10.1523/jneurosci.0305-20.2020.

Barnett L, Seth AK. The MVGC multivariate granger causality toolbox: a new approach to granger-causal inference. *J Neurosci Methods*. 2014:223:50–68. https://doi.org/10.1016/j.jneumeth.2013.10.018.

Benchenane K, Peyrache A, Khamassi M, Tierney PL, Gioanni Y, Battaglia FP, Wiener SI. Coherent theta oscillations and reorganization of spike timing in the hippocampal- prefrontal network upon learning. *Neuron*. 2010:66(6):921–936. https://doi.org/10.1016/j.neuron.2010.05.013.

Bohbot VD, Kalina M, Stepankova K, Spackova N, Petrides M, Nadel L. Spatial memory deficits in patients with lesions to the right hippocampus and to the right parahippocampal cortex. *Neuropsychologia*. 1998:36(11):1217–1238. https://doi.org/10.1016/s0028-3932(97)00161-9.

Brincat SL, Miller EK. Frequency-specific hippocampal-prefrontal interactions during associative learning. *Nat Neurosci*. 2015:18(4):576–581. https://doi.org/10.1038/nn.3954.

Brovelli A, Ding M, Ledberg A, Chen Y, Nakamura R, Bressler SL. Beta oscillations in a large-scale sensorimotor cortical network: directional influences revealed by granger causality. *Proc Natl Acad Sci U S A*. 2004:101(26):9849–9854. https://doi.org/10.1073/pnas.0308538101.

Buckner RL, Wheeler ME. The cognitive neuroscience of remembering. *Nat Rev Neurosci*. 2001:2(9):624–634. https://doi.org/10.1038/35090048.

Burgess N, Maguire EA, Spiers HJ, O'Keefe J. A temporoparietal and prefrontal network for retrieving the spatial context of lifelike events. *NeuroImage*. 2001:14(2):439–453. https://doi.org/10.1006/nimg.2001.0806.

Burgess N, Maguire EA, O'Keefe J. The human hippocampus and spatial and episodic memory. *Neuron*. 2002:35(4):625–641. https://doi.org/10.1016/s0896-6273(02)00830-9.

Burke JF, Zaghloul KA, Jacobs J, Williams RB, Sperling MR, Sharan AD, Kahana MJ. Synchronous and asynchronous theta and gamma activity during episodic memory formation. *J Neurosci*. 2013:33(1):292–304. https://doi.org/10.1523/JNEUROSCI.2057-12.2013.

Buzsáki G. Theta rhythm of navigation: link between path integration and landmark navigation, episodic and semantic memory. *Hippocampus*. 2005:15(7):827–840. https://doi.org/10.1002/hipo.20113.

Canolty RT, Knight RT. The functional role of cross-frequency coupling. *Trends Cogn Sci*. 2010:14(11):506–515. https://doi.org/10.1016/j.tics.2010.09.001.

Coughlan G, Laczó J, Hort J, Minihane AM, Hornberger M. Spatial navigation deficits - overlooked cognitive marker for

preclinical Alzheimer disease? *Nat Rev Neurol*. 2018:14(8):496–506. https://doi.org/10.1038/s41582-018-0031-x.

Das A, Menon V. Spatiotemporal integrity and spontaneous nonlinear dynamic properties of the salience network revealed by human intracranial electrophysiology: a multicohort replication. *Cereb Cortex*. 2020:30(10):5309–5321. 10.1093/cercor/bhaa111.

Das A, Menon V. Asymmetric frequency-specific feedforward and feedback information flow between hippocampus and prefrontal cortex during verbal memory encoding and recall. *J Neurosci*. 2021:41(40):8427–8440.

Dobbins IG, Foley H, Schacter DL, Wagner AD. Executive control during episodic retrieval: multiple prefrontal processes subserve source memory. *Neuron*. 2002:35(5):989–996. https://doi.org/10.1016/s0896-6273(02)00858-9.

Eichenbaum H. Prefrontal-hippocampal interactions in episodic memory. *Nat Rev Neurosci*. 2017:18(9):547–558. https://doi.org/10.1038/nrn.2017.74.

Eichenbaum H, Dudchenko P, Wood E, Shapiro M, Tanila H. The hippocampus, memory, and place cells: is it spatial memory or a memory space? *Neuron*. 1999:23(2):209–226. https://doi.org/10.1016/s0896-6273(00)80773-4.

Ekstrom AD, Watrous AJ. Multifaceted roles for low-frequency oscillations in bottom-up and top-down processing during navigation and memory. *NeuroImage*. 2014:85(Pt 2):667–677. https://doi.org/10.1016/j.neuroimage.2013.06.049.

Ekstrom AD, Kahana MJ, Caplan JB, Fields TA, Isham EA, Newman EL, Fried I. Cellular networks underlying human spatial navigation. *Nature*. 2003:425(6954):184–188. https://doi.org/10.1038/nature01964.

Ekstrom AD, Huffman DJ, Starrett M. Interacting networks of brain regions underlie human spatial navigation: a review and novel synthesis of the literature. *J Neurophysiol*. 2017:118(6):3328–3344. https://doi.org/10.1152/jn.00531.2017.

Engel AK, Fries P. Beta-band oscillations–signalling the status quo? *Curr Opin Neurobiol*. 2010:20(2):156–165. https://doi.org/10.1016/j.conb.2010.02.015.

Epstein RA, Patai EZ, Julian JB, Spiers HJ. The cognitive map in humans: spatial navigation and beyond. *Nat Neurosci*. 2017:20(11):1504–1513. https://doi.org/10.1038/nn.4656.

Ezzyat Y, Wanda PA, Levy DF, Kadel A, Aka A, Pedisich I, Kahana MJ. Closed-loop stimulation of temporal cortex rescues functional networks and improves memory. *Nat Commun*. 2018:9(1):365. https://doi.org/10.1038/s41467-017-02753-0.

Fan L, Li H, Zhuo J, Zhang Y, Wang J, Chen L, Jiang T. The human Brainnetome atlas: a new brain atlas based on connectional architecture. *Cereb Cortex*. 2016:26(8):3508–3526. https://doi.org/10.1093/cercor/bhw157.

Fontolan L, Morillon B, Liegeois-Chauvel C, Giraud AL. The contribution of frequency-specific activity to hierarchical information processing in the human auditory cortex. *Nat Commun*. 2014:5:4694. https://doi.org/10.1038/ncomms5694.

Ghaem O, Mellet E, Crivello F, Tzourio N, Mazoyer B, Berthoz A, Denis M. Mental navigation along memorized routes activates the hippocampus, precuneus, and insula. *Neuroreport*. 1997:8(3):739–744. https://doi.org/10.1097/00001756-199702100-00032.

Goyal A, Miller J, Watrous AJ, Lee SA, Coffey T, Sperling MR, Jacobs J. Electrical stimulation in hippocampus and entorhinal cortex impairs spatial and temporal memory. *J Neurosci*. 2018:38(19):4471–4481. https://doi.org/10.1523/JNEUROSCI.3049-17.2018.

Greicius MD, Krasnow B, Boyett-Anderson JM, Eliez S, Schatzberg AF, Reiss AL, Menon V. Regional analysis of hippocampal activation during memory encoding and retrieval: fMRI study. *Hippocampus*. 2003:13(1):164–174. https://doi.org/10.1002/hipo.10064.

Grön G, Wunderlich AP, Spitzer M, Tomczak R, Riepe MW. Brain activation during human navigation: gender-different neural networks as substrate of performance. *Nat Neurosci*. 2000:3(4):404–408. https://doi.org/10.1038/73980.

Hartley T, Lever C, Burgess N, O'Keefe J. Space in the brain: how the hippocampal formation supports spatial cognition. *Philos Trans R Soc Lond Ser B Biol Sci*. 2014:369(1635):20120510. https://doi.org/10.1098/rstb.2012.0510.

Hasegawa I, Hayashi T, Miyashita Y. Memory retrieval under the control of the prefrontal cortex. *Ann Med*. 1999:31(6):380–387. https://doi.org/10.3109/07853899908998795.

Hebscher M, Gilboa A. A boost of confidence: the role of the ventromedial prefrontal cortex in memory, decision-making, and schemas. *Neuropsychologia*. 2016:90:46–58. https://doi.org/10.1016/j.neuropsychologia.2016.05.003.

Hebscher M, Meltzer JA, Gilboa A. A causal role for the precuneus in network-wide theta and gamma oscillatory activity during complex memory retrieval. *elife*. 2019:8. https://doi.org/10.7554/eLife.43114.

Herweg NA, Kahana MJ. Spatial representations in the human brain. *Front Hum Neurosci*. 2018:12:297. https://doi.org/10.3389/fnhum.2018.00297.

Hillebrand A, Tewarie P, van Dellen E, Yu M, Carbo EW, Douw L, Stam CJ. Direction of information flow in large-scale resting-state networks is frequency-dependent. *Proc Natl Acad Sci U S A*. 2016:113(14):3867–3872. https://doi.org/10.1073/pnas.1515657113.

Hutchison RM, Hashemi N, Gati JS, Menon RS, Everling S. Electrophysiological signatures of spontaneous BOLD fluctuations in macaque prefrontal cortex. *NeuroImage*. 2015:113:257–267. https://doi.org/10.1016/j.neuroimage.2015.03.062.

Iglói K, Doeller CF, Berthoz A, Rondi-Reig L, Burgess N. Lateralized human hippocampal activity predicts navigation based on sequence or place memory. *Proc Natl Acad Sci U S A*. 2010:107(32):14466–14471. https://doi.org/10.1073/pnas.1004243107.

Jacobs J, Weidemann CT, Miller JF, Solway A, Burke JF, Wei XX, Kahana MJ. Direct recordings of grid-like neuronal activity in human spatial navigation. *Nat Neurosci*. 2013:16(9):1188–1190. https://doi.org/10.1038/nn.3466.

Jacobs J, Miller J, Lee SA, Coffey T, Watrous AJ, Sperling MR, Rizzuto DS. Direct electrical stimulation of the human entorhinal region and hippocampus impairs memory. *Neuron*. 2016:92(5):983–990. https://doi.org/10.1016/j.neuron.2016.10.062.

Javadi AH, Emo B, Howard LR, Zisch FE, Yu Y, Knight R, Spiers HJ. Hippocampal and prefrontal processing of network topology to simulate the future. *Nat Commun*. 2017:8:14652. https://doi.org/10.1038/ncomms14652.

Jeffreys H. *The theory of probability*. 3rd ed. Oxford, England: Oxford University Press; 1998

Jones MW, Wilson MA. Theta rhythms coordinate hippocampal-prefrontal interactions in a spatial memory task. *PLoS Biol*. 2005:3(12):e402. https://doi.org/10.1371/journal.pbio.0030402.

Kaplan R, Doeller CF, Barnes GR, Litvak V, Düzel E, Bandettini PA, Burgess N. Movement-related theta rhythm in humans: coordinating self-directed hippocampal learning. *PLoS Biol*. 2012:10(2):e1001267. https://doi.org/10.1371/journal.pbio.1001267.

Kaplan R, Horner AJ, Bandettini PA, Doeller CF, Burgess N. Human hippocampal processing of environmental novelty during spatial navigation. *Hippocampus*. 2014:24(7):740–750. https://doi.org/10.1002/hipo.22264.

Kayser C, Montemurro MA, Logothetis NK, Panzeri S. Spike-phase coding boosts and stabilizes information carried by spatial and temporal spike patterns. *Neuron*. 2009:61(4):597–608. https://doi.org/10.1016/j.neuron.2009.01.008.

Kim SM, Ganguli S, Frank LM. Spatial information outflow from the hippocampal circuit: distributed spatial coding and phase precession in the subiculum. *J Neurosci*. 2012:32(34):11539–11558. https://doi.org/10.1523/jneurosci.5942-11.2012.

Kuznetsova A, Brockhoff PB, Christensen RHB. lmerTest package: tests in linear mixed effects models. *J Stat Softw*. 2017:82(13):1–26.

Lachaux JP, Rodriguez E, Martinerie J, Varela FJ. Measuring phase synchrony in brain signals. *Hum Brain Mapp*. 1999:8(4):194–208. https://doi.org/10.1002/(sici)1097-0193(1999)8:4<194::aid-hbm4>3.0.co;2-c.

Lakatos P, Gross J, Thut G. A new unifying account of the roles of neuronal entrainment. *Curr Biol*. 2019:29(18):R890–R905. https://doi.org/10.1016/j.cub.2019.07.075.

Lee SA, Miller JF, Watrous AJ, Sperling MR, Sharan A, Worrell GA, Jacobs J. Electrophysiological signatures of spatial boundaries in the human subiculum. *J Neurosci*. 2018:38(13):3265–3272. https://doi.org/10.1523/jneurosci.3216-17.2018.

Leopold DA, Murayama Y, Logothetis NK. Very slow activity fluctuations in monkey visual cortex: implications for functional brain imaging. *Cereb Cortex*. 2003:13(4):422–433. https://doi.org/10.1093/cercor/13.4.422.

Lobier M, Siebenhühner F, Palva S, Matias PJ. Phase transfer entropy: a novel phase-based measure for directed connectivity in networks coupled by oscillatory interactions. *NeuroImage*. 2014:85:853–872. https://doi.org/10.1016/j.neuroimage.2013.08.056.

Long NM, Burke JF, Kahana MJ. Subsequent memory effect in intracranial and scalp EEG. *NeuroImage*. 2014:84:488–494. https://doi.org/10.1016/j.neuroimage.2013.08.052.

Lopour BA, Tavassoli A, Fried I, Ringach DL. Coding of information in the phase of local field potentials within human medial temporal lobe. *Neuron*. 2013:79(3):594–606. https://doi.org/10.1016/j.neuron.2013.06.001.

Ly A, Etz A, Marsman M, Wagenmakers EJ. Replication Bayes factors from evidence updating. *Behav Res Methods*. 2019:51(6):2498–2508. https://doi.org/10.3758/s13428-018-1092-x.

Maguire EA, Burke T, Phillips J, Staunton H. Topographical disorientation following unilateral temporal lobe lesions in humans. *Neuropsychologia*. 1996:34(10):993–1001. https://doi.org/10.1016/0028-3932(96)00022-x.

Maguire EA, Burgess N, Donnett JG, Frackowiak RS, Frith CD, O'Keefe J. Knowing where and getting there: a human navigation network. *Science*. 1998:280(5365):921–924. https://doi.org/10.1126/science.280.5365.921.

Maguire EA, Burgess N, O'Keefe J. Human spatial navigation: cognitive maps, sexual dimorphism, and neural substrates. *Curr Opin Neurobiol*. 1999:9(2):171–177. https://doi.org/10.1016/s0959-4388(99)80023-3.

Maguire EA, Gadian DG, Johnsrude IS, Good CD, Ashburner J, Frackowiak RS, Frith CD. Navigation-related structural change in the hippocampi of taxi drivers. *Proc Natl Acad Sci U S A*. 2000:97(8):4398–4403. https://doi.org/10.1073/pnas.070039597.

Mantini D, Perrucci MG, Del Gratta C, Romani GL, Corbetta M. Electrophysiological signatures of resting state networks in the human brain. *Proc Natl Acad Sci U S A*. 2007:104(32):13170–13175. https://doi.org/10.1073/pnas.0700668104.

Menon V, Freeman WJ, Cutillo BA, Desmond JE, Ward MF, Bressler SL, Gevins AS. Spatio-temporal correlations in human gamma band electrocorticograms. *Electroencephalogr Clin Neurophysiol*. 1996:98(2):89–102. https://doi.org/10.1016/0013-4694(95)00206-5.

Miller EK, Cohen JD. An integrative theory of prefrontal cortex function. *Annu Rev Neurosci*. 2001:24:167–202. https://doi.org/10.1146/annurev.neuro.24.1.167.

Miller J, Watrous AJ, Tsitsiklis M, Lee SA, Sheth SA, Schevon CA, Jacobs J. Lateralized hippocampal oscillations underlie distinct aspects of human spatial memory and navigation. *Nat Commun*. 2018:9(1):2423. https://doi.org/10.1038/s41467-018-04847-9.

Moreno A, Morris RGM, Canals S. Frequency-dependent gating of hippocampal-neocortical interactions. *Cereb Cortex*. 2016:26(5):2105–2114. https://doi.org/10.1093/cercor/bhv033.

Morris R. Developments of a water-maze procedure for studying spatial learning in the rat. *J Neurosci Methods*. 1984:11(1):47–60. https://doi.org/10.1016/0165-0270(84)90007-4.

Moscovitch M. Memory and working-with-memory: a component process model based on modules and central systems. *J Cogn Neurosci*. 1992:4(3):257–267. https://doi.org/10.1162/jocn.1992.4.3.257.

Negrón-Oyarzo I, Espinosa N, Aguilar-Rivera M, Fuenzalida M, Aboitiz F, Fuentealba P. Coordinated prefrontal-hippocampal activity and navigation strategy-related prefrontal firing during spatial memory formation. *Proc Natl Acad Sci U S A*. 2018:115(27):7123–7128. https://doi.org/10.1073/pnas.1720117115.

Neuner I, Arrubla J, Werner CJ, Hitz K, Boers F, Kawohl W, Shah NJ. The default mode network and EEG regional spectral power: a simultaneous fMRI-EEG study. *PLoS One*. 2014:9(2):e88214. https://doi.org/10.1371/journal.pone.0088214.

Ng BS, Logothetis NK, Kayser C. EEG phase patterns reflect the selectivity of neural firing. *Cereb Cortex*. 2013:23(2):389–398. https://doi.org/10.1093/cercor/bhs031.

O'Keefe J, Conway DH. Hippocampal place units in the freely moving rat: why they fire where they fire. *Exp Brain Res*. 1978:31(4):573–590. https://doi.org/10.1007/bf00239813.

Peterson RA, Cavanaugh JE. Ordered quantile normalization: a semiparametric transformation built for the cross-validation era. *J Appl Stat*. 2018:82(13–15):2312–2327.

Place R, Farovik A, Brockmann M, Eichenbaum H. Bidirectional prefrontal-hippocampal interactions support context-guided memory. *Nat Neurosci*. 2016:19(8):992–994. https://doi.org/10.1038/nn.4327.

Postle BR. Working memory as an emergent property of the mind and brain. *Neuroscience*. 2006:139(1):23–38. https://doi.org/10.1016/j.neuroscience.2005.06.005.

Pu Y, Cornwell BR, Cheyne D, Johnson BW. The functional role of human right hippocampal/parahippocampal theta rhythm in environmental encoding during virtual spatial navigation. *Hum Brain Mapp*. 2017:38(3):1347–1361. https://doi.org/10.1002/hbm.23458.

Rouder JN, Speckman PL, Sun D, Morey RD, Iverson G. Bayesian t tests for accepting and rejecting the null hypothesis. *Psychon Bull Rev*. 2009:16(2):225–237. https://doi.org/10.3758/pbr.16.2.225.

Roy A, Svensson FP, Mazeh A, Kocsis B. Prefrontal-hippocampal coupling by theta rhythm and by 2-5 Hz oscillation in the delta band: the role of the nucleus reuniens of the thalamus. *Brain Struct Funct*. 2017:222(6):2819–2830. https://doi.org/10.1007/s00429-017-1374-6.

Rutishauser U, Reddy L, Mormann F, Sarnthein J. The architecture of human memory: insights from human single-neuron recordings. *J Neurosci*. 2021:41(5):883–890. https://doi.org/10.1523/jneurosci.1648-20.2020.

Scheuble V, Beauducel A. Cognitive processes during deception about attitudes revisited: a replication study. *Soc Cogn Affect Neurosci*. 2020:15(8):839–848. https://doi.org/10.1093/scan/nsaa107.

Schoffelen JM, Hulten A, Lam N, Marquand AF, Udden J, Hagoort P. Frequency-specific directed interactions in the human brain network for language. *Proc Natl Acad Sci U S A*. 2017:114(30):8083–8088. https://doi.org/10.1073/pnas.1703155114.

Scholvinck ML, Maier A, Ye FQ, Duyn JH, Leopold DA. Neural basis of global resting-state fMRI activity. *Proc Natl Acad*

Sci U S A. 2010:107(22):10238–10243. https://doi.org/10.1073/pnas.0913110107.

Schultheiss NW, Schlecht M, Jayachandran M, Brooks DR, McGlothan JL, Guilarte TR, Allen TA. Awake delta and theta-rhythmic hippocampal network modes during intermittent locomotor behaviors in the rat. *Behav Neurosci*. 2020:134(6):529–546. https://doi.org/10.1037/bne0000409.

Siapas AG, Lubenov EV, Wilson MA. Prefrontal phase locking to hippocampal theta oscillations. *Neuron*. 2005:46(1):141–151. https://doi.org/10.1016/j.neuron.2005.02.028.

Siegel M, Warden MR, Miller EK. Phase-dependent neuronal coding of objects in short-term memory. *Proc Natl Acad Sci U S A*. 2009:106(50):21341–21346. https://doi.org/10.1073/pnas.0908193106.

Simons JS, Spiers HJ. Prefrontal and medial temporal lobe interactions in long-term memory. *Nat Rev Neurosci*. 2003:4(8):637–648. https://doi.org/10.1038/nrn1178.

Smith ML, Milner B. Right hippocampal impairment in the recall of spatial location: encoding deficit or rapid forgetting? *Neuropsychologia*. 1989:27(1):71–81. https://doi.org/10.1016/0028-3932(89)90091-2.

Solomon EA, Stein JM, Das S, Gorniak R, Sperling MR, Worrell G, Kahana MJ. Dynamic theta networks in the human medial temporal lobe support episodic memory. *Curr Biol*. 2019:29(7):1100–1111.e1104. https://doi.org/10.1016/j.cub.2019.02.020.

Spiers HJ. Brain rhythms that help us to detect borders. *Nature*. 2020:589:353–354. https://doi.org/10.1038/d41586-020-03576-8.

Spiers HJ, Maguire EA. Thoughts, behaviour, and brain dynamics during navigation in the real world. *NeuroImage*. 2006:31(4):1826–1840. https://doi.org/10.1016/j.neuroimage.2006.01.037.

Spiers HJ, Burgess N, Maguire EA, Baxendale SA, Hartley T, Thompson PJ, O'Keefe J. Unilateral temporal lobectomy patients show lateralized topographical and episodic memory deficits in a virtual town. *Brain*. 2001:124(Pt 12):2476–2489. https://doi.org/10.1093/brain/124.12.2476.

Spitzer B, Haegens S. Beyond the status quo: a role for Beta oscillations in endogenous content (re)activation. *eNeuro*. 2017:4(4). https://doi.org/10.1523/eneuro.0170-17.2017.

Stangl M, Topalovic U, Inman CS, Hiller S, Villaroman D, Aghajan ZM, Suthana N. Boundary-anchored neural mechanisms of location-encoding for self and others. *Nature*. 2021:589(7842):420–425. https://doi.org/10.1038/s41586-020-03073-y.

Stanley DA, Roy JE, Aoi MC, Kopell NJ, Miller EK. Low-Beta oscillations turn up the gain during category judgments. *Cereb Cortex*. 2018:28(1):116–130. https://doi.org/10.1093/cercor/bhw356.

Stevenson RF, Zheng J, Mnatsakanyan L, Vadera S, Knight RT, Lin JJ, Yassa MA. Hippocampal CA1 gamma power predicts the precision of spatial memory judgments. *Proc Natl Acad Sci U S A*. 2018:115(40):10148–10153. https://doi.org/10.1073/pnas.1805724115.

Tang W, Shin JD, Frank LM, Jadhav SP. Hippocampal-prefrontal reactivation during learning is stronger in awake compared with sleep states. *J Neurosci*. 2017:37(49):11789–11805. https://doi.org/10.1523/jneurosci.2291-17.2017.

Tsitsiklis M, Miller J, Qasim SE, Inman CS, Gross RE, Willie JT, Jacobs J. Single-neuron representations of spatial targets in humans. *Curr Biol*. 2020:30(2):245–253.e244. https://doi.org/10.1016/j.cub.2019.11.048.

Verhagen J, Wagenmakers EJ. Bayesian tests to quantify the result of a replication attempt. *J Exp Psychol Gen*. 2014:143(4):1457–1475. https://doi.org/10.1037/a0036731.

Wagner AD, Pare-Blagoev EJ, Clark J, Poldrack RA. Recovering meaning: left prefrontal cortex guides controlled semantic retrieval. *Neuron*. 2001:31(2):329–338. https://doi.org/10.1016/s0896-6273(01)00359-2.

Wang MY, Wang J, Zhou J, Guan YG, Zhai F, Liu CQ, Luan GM. Identification of the epileptogenic zone of temporal lobe epilepsy from stereo-electroencephalography signals: a phase transfer entropy and graph theory approach. *Neuroimage Clin*. 2017:16:184–195. https://doi.org/10.1016/j.nicl.2017.07.022.

Watrous AJ, Tandon N, Conner CR, Pieters T, Ekstrom AD. Frequency-specific network connectivity increases underlie accurate spatiotemporal memory retrieval. *Nat Neurosci*. 2013:16(3):349–356. https://doi.org/10.1038/nn.3315.

Wirth S, Yanike M, Frank LM, Smith AC, Brown EN, Suzuki WA. Single neurons in the monkey hippocampus and learning of new associations. *Science*. 2003:300(5625):1578–1581. https://doi.org/10.1126/science.1084324.

Zielinski MC, Shin JD, Jadhav SP. Coherent coding of spatial position mediated by theta oscillations in the hippocampus and prefrontal cortex. *J Neurosci*. 2019:39(23):4550–4565. https://doi.org/10.1523/jneurosci.0106-19.2019.